

intermean



(1)

AD A951570

SYNTHETIC RADAR ECHOES IN THE PRESENCE OF JAMMING

2311

NOTE: This document contains information affecting the National Defense of the United States within the meaning of the Espionage Act (U. S. C. 50: 31, 32). The transmission of this document or the revelation of its contents in any manner to an unauthorized person is prohibited by law.

NAVAL RESEARCH
LABORATORY, WASH. D.C.

JUL 4 10 54 AM 1945

98

RECEIVED
MAIN OFFICE

REPORT
708

DTIC
ELECT

DEC 1 1 1945

Classification changed from *Secret*
To *Unclassified*
By authority of *C. A. L. Sec. 9125 P44*
File No. *7913-A21/54x* Dated *11 Feb 1986*

A
RECEIVED

RADIATION LABORATORY
MASSACHUSETTS INSTITUTE OF TECHNOLOGY
CAMBRIDGE MASSACHUSETTS

AUG 26 1958

LIBRARY
NAVAL RESEARCH LABORATORY

This document has been approved for public release and sale, its distribution is unlimited.

Form with fields for NTIS, DTIC, Unann., and other administrative markings. Includes handwritten 'A 93' and a circular stamp.

UNANNOUNCED

BEST AVAILABLE COPY

81

MEMO
Div. 7A
OBER-262

Mediation Laboratory

Report 706

June 22, 1945

SYNTHETIC RADAR ECHOES IN THE PRESENCE OF JAMMING

Abstract

This report contains the result of some experiments to determine the deleterious effects of certain kinds of jamming on the visibility of radar echoes. The jamming signals employed were: (1) CW at the radar carrier frequency; and (2) CW amplitude-modulated by relatively pure noise under various conditions of clipping and bandwidth. In a later report will appear the results for frequency modulation by noise.

A bench assembly was used, consisting of an artificial radar echo, an artificial jamming signal, a method of mixing the two and finally a receiver of variable bandwidth and a conventional type A display. Every attempt was made to keep the result quantitative throughout. In particular, a rather elaborate statistical method of establishing the signal threshold was devised, in order to avoid the ambiguities inherent in the hitherto customary method of determining the threshold by a psychological evaluation of minimum discernibility. Furthermore a method of referring all power levels to receiver noise power was employed. It was found that the deterioration in visibility could be said to depend mainly on the following independent variables: (1) i-f bandwidth, (2) jamming carrier strength, (3) percent modulation, (4) noise bandwidth. Curves are presented to show the effect of varying these parameters, but the results may be succinctly stated in the following manner. The signal threshold in the absence of jamming is determined by the ratio of signal power to receiver noise power. Then the impairment of visibility by jamming can be estimated by adding to the receiver noise power an amount of additional i-f noise calculated in simple terms from the jamming carrier strength, percent modulation, noise bandwidth, and i-f bandwidth. To this should be added 3-4 db to take into account the effect of the CW carrier. From this value, however, should be subtracted an amount that depends on the amount of clipping of the jamming noise. This amount depends upon the ratio of i-f to jamming noise bandwidths and modulation index; typical values are, perhaps, 3-6 db.

The experimental work in this report was completed in 1943.

A. M. Stone

Approved by

James L. Lawson
Leader, Group 44

J. J. Rohr
Squad, Division 4

Title page
33 numbered pages
21 pages of figures

~~SECRET~~

TABLE OF CONTENTS

I.	INTRODUCTION	2
A.	Definition and Scope of Problem	2
B.	Definition and Scope of Problem (cont.)	2
C.	Definition and Scope of Problem (cont.)	3
II.	PREVIOUS EXPERIMENTS AND THEORY	3
A.	Theory.	4
B.	Experiment	6
III.	EXPERIMENTAL ARRANGEMENT AND PROCEDURE	5
A.	Block Diagram	5
B.	Procedure	9
C.	Technique of Assembling Data	11
IV.	EXPERIMENTAL RESULTS	13
A.	Effect of CW	13
B.	Jamming Effectiveness as a Function of I-f Bandwidth and Pulse Length	15
C.	The Effect of Increase in Jamming Strength	18
D.	Effect of Modulation Index	19
E.	Variation of Jamming Noise Bandwidth	21
F.	Clipping Factors	23
G.	Signal Threshold vs. Jamming Power	25
H.	Signal Threshold Dependence on Pulse Lengths	25
I.	Restrictions on Results	26
V.	SUMMARY OF RESULTS AND CONCLUSIONS	26
A.	Antijamming Measures	26
B.	Quantitative Estimate of Jamming Power	27
C.	Acknowledgement	28
	References	29
	Appendix A	30
	Appendix B	32

~~CONFIDENTIAL~~
SCIENTIFIC RADAR SIGNALS IN THE PRESENCE OF JAMMING

PART I AMPLITUDE MODULATION BY NOISE

1 INTRODUCTION

A Definition and Scope of Problem

A rigid definition of the "visibility" of a radar echo is elusive. Whatever quantitative arbitrary standard is proposed for this quality, however, it will certainly be found to depend upon a host of more or less independent variables or parameters connected not only with the radar system, but also with external conditions as well. In the light of these fifty or so quantities (which have been listed in Appendix A), this report is primarily concerned with a comparatively minute, yet important, segment of the problem of the "detectability" of radar signals.

In short, this report is concerned primarily with a study of the effects of interference, or jamming, signals on the discernibility of true radar echoes. In the present work we restrict ourselves in the main to the study of interfering signals consisting of an r-f carrier amplitude-modulated by "resistor noise", or its equivalent. Such specialization may appear unwarranted but it appears from both theoretical considerations and laboratory experiments that AM by noise jamming and FM by noise jamming -- that latter will constitute a later Part II of these studies -- are two of the most serious interference effects expected from the AJ standpoint. Furthermore this entire investigation has been limited to a consideration of the masking effects of jamming on signals presented on a Type A oscilloscope: it is likely, within limits discussed below, that the results, at least partially, are applicable to other type of presentation. Similarly, values of all other radar parameters not varied have been set at arbitrary, but operationally useful, levels. These will be the subject of detailed comments in the appropriate sections. By dint of this procedure it is hoped that the results presented will be typical of a fairly large class of representative radar systems.

B Definition and Scope of Problem (cont.)

There are, to be sure, conceptually many different forms of jamming; for some of these anti-jamming palliatives immediately suggest themselves or the efficiency of jamming is low. C-w interference, low frequency sine wave modulation of a carrier, either in the form of AM or FM, some types of "railing" type interference belong to this latter low efficiency class*, and therefore are

* None of these types of jamming is of low efficiency if it overloads any part of the receiving system. In the experiments and discussion to follow, all questions of overload are avoided.

~~CONFIDENTIAL~~

Some modulation, of either of the types mentioned does present on the oscilloscope screen a pattern both uniform and uniformly complex enough so that its effects are little distinguishable from that of receiver noise itself. Thus, for most intents and purposes, one may assume that no AJ palliative can be applied, once the interfering signal is permitted to arrive at the receiver terminals, other than to adjust the various system parameters for optimum performance in the presence of the particular type of jamming employed. This work, then, will find its chief usefulness in indicating what the optimum arrangement is under different conditions of jamming and in determining how serious the jamming actually is.

The so-called DINA jamming scheme ("direct noise amplification") is not at present a major concern at microwavelengths because of the hitherto inherent difficulty of producing pure noise of sufficient power in this spectral region⁽¹⁾. For this reason, and for the reason that DINA effects can probably be calculated directly from studies on receiver noise this phase of the problem has not been studied.

C. Definition and Scope of the Problem (cont.)

Fundamentally, one wishes to preserve, in the presence of enemy jamming, the maximum amount of information obtainable from a radar echo; this involves range and bearing, as complete discrimination as possible between moving and ground targets, a maximum of resolution between true and false echoes. It may be noted that, if the jammer is attempting to screen himself, bearing information is automatically given the radar operator. But these desiderata are influenced by nothing very different from the parameters that influence a radar set performance in the absence of jamming. Since the external noise jammer has, with some limitations, merely the effect of increasing the receiver's overall noise figure, the same considerations that apply in the latter case can be largely carried over to the former.

II PREVIOUS THEORY AND EXPERIMENTS

It is advisable to review, in brief fashion, some of the ideas that have recently been developed with regard to the visibility of signals in receiver noise. The conclusions stated here will be assessed in Section IV in an attempt to understand the experimental results therein presented. For the sake of Brevity, none of the arguments leading to the stated conclusions are presented.

* The possibility of the future use of single sideband carrier-suppressed modulation must not be overlooked.

~~SECRET~~

A theoretical study has been made by Uhlenbeck on the problem of signal discernibility in the presence of receiver noise. From a private report of this and from the earlier work of Goudsmit⁽²⁾, Goudsmit and Weiss⁽³⁾, North⁽⁴⁾, Jordan⁽⁵⁾, and others, the following salient features may be gleaned.

(1) Signal visibility is essentially a study in probability. The noise peaks visible on the type A oscilloscope are distributed in amplitude according to a certain probability law: the presence of the signal modifies that law locally, and this modification is (sometimes!) recognized as the signal. The probability distributions of noise peaks as a function of the signal power have been obtained for the case of a linear detector in the references cited. From these curves (taking into account the pulse shape) the behavior of the minimum discernible signal, or the signal threshold (hereinafter to be denoted by S_t), as a function of the receiver i-f bandwidth can be calculated. An optimum i-f bandwidth, i.e., one requiring the smallest signal power for discernibility, can be found; it is approximately equal to the reciprocal of the pulse length. In regions far from the maximum, S_t is proportional to the i-f bandwidth on the high side; it is proportional to the reciprocal of the i-f bandwidth on the low side.

(2) Certain scaling arguments can be introduced. For example, one such argument is that, if τ is the pulse length; B , the i-f bandwidth; b , the video bandwidth, and if the sweep speed is adjusted in every case to keep the same geometrical relationships on the oscilloscope screen, then

$$S_t \tau = F(B \cdot \tau) \quad G(b \cdot \tau) \quad (1)$$

where F and G are functions which have been determined by experiment, and also, in some cases, have been derived from theory. Thus the longer the pulse the smaller the signal threshold at any particular value of $B \cdot \tau$.

(3) For an "ideal" observer, Uhlenbeck has found that

$$S_t = \frac{f(B, b, \tau, \text{etc.})}{N^2} \quad (11)$$

where N is the total number of sweeps containing signal and noise, equal to the pulse repetition frequency multiplied by the signal presentation time

~~SECRET~~

SECTION 04

(1) receptor phenomena (1), have been confirmed by Lawson, Sydnorak, et al over an extremely wide range. In addition their investigations have included the study of psychological factors affecting the visibility of small signals for example, the effect of ambient light, operator training, etc

(2) Experiments by Haerf⁽⁶⁾ have led him to an empirical formula for the minimum discernible signal, viz

$$S_t = R^2 \left(1 + \frac{1}{R^2} \right) \quad (111)$$

How this empirical formula compares with the present experimental results will be shown in Section IV

(3) A report by Taylor and Peterson⁽⁷⁾ appeared while the present work was in progress. In this report the signal discernibility in the presence of jamming was considered. Jamming signals were AM by noise and low frequency sine wave modulation. The present report is supplementary and additive to the results of Peterson and Taylor in that a systematic study of a few of the variables entering the problem has been made

III EXPERIMENTAL ARRANGEMENT AND PROCEDURE

In order to appreciate the results of this investigation a rather complete account of the experimental apparatus will be given

A Block Diagram

A block diagram of the entire experimental arrangement is shown in Fig. 1. In the left-hand side of Fig. 1 is shown a box labelled "noise source". This is a primary source of resistance noise, followed by a video amplifier. The output of this amplifier modulates the grid of the klystron amplifier; this klystron amplifier in turn is driven by the klystron oscillator as shown. The interference signal is then obtained from the output of the klystron amplifier AM by noise* and fed into the receiver through a calibrated attenuator. At the same time an artificial echo, manufactured in the apparatus labelled "pulse signal generator", is fed through its attenuator likewise into the receiver. The type oscilloscope, on which the receiver output is viewed, is a slightly altered J4 Synchronoscope. Losses/padding was appropriately distributed as shown on the block diagram of Fig. 1.

* "AM by noise" is used as an abbreviation for "amplitude modulation by an external source of noise"

~~SECRET~~

The rest of the apparatus indicated in Fig. 1 consists of (a) a meter to measure the output of the noise source; (b) a monitoring crystal to check on the r-f output of the klystron amplifier; (c) a spectrum analyzer to monitor both the noise and interfering signals; and (d) an r-f oscillator whose function will be disclosed below.

(2) The noise source is an integral and important part of the apparatus, and its proper design is essential for an unambiguous interpretation of the results. No particular research was done on the optimum primary source of noise. A 931 RCA photomultiplier tube (later superseded by a selected version of the same, the 1P21) was currently considered the best available primary source and thus was chosen for use. The manufacturer's rating of output capacitance was sufficiently low so as to place only secondary limitation here on the bandwidth of the noise output available from the noise source. (Some results of Cobine⁽⁸⁾ show that the RCA 884 thyratron, also sometimes suggested for use as a primary source of noise, has a noise spectrum of considerably less uniformity than the 931 tube^{*}; Sard⁽¹⁾ has shown theoretically that the spectrum of the noise output of the 931 alone should be uniform and flat out to about 500 Mc/sec while Cobine⁽⁹⁾ has experimental data showing that, with 200 volts per stage and 0.6 ma output current (d-c) the noise spectrum is flat out to at least beyond 5 Mc/sec which was as far as the measurements were carried.

The widest video bandwidth of the noise source desired was of the order of 6 Mc/sec measured at the half-power points. At the same time a gain of some 60 db or more was needed to get adequate output noise power from the 931 tube. The video amplifier finally used in conjunction with the photomultiplier tube is shown schematically in Figs. 2a and 2b. Cathode peaking was used in each stage. The entire amplifier was tested with microsecond pulses and showed the proper behavior. The amplitude response curve, minus the output stage of the 931 tube, as measured by a calibrated oscillator and General Radio vacuum tube voltmeter, is shown in Fig. 7. The overall bandwidth in the widest case is seen to be 6.3 Mc/sec. Including the 931 tube, the effective overall bandwidth is about 5.5 Mc/sec. Good low frequency response was ensured by the large time constant in each coupling circuit. There was no detectable power frequency hum in the output.

* We have noticed the same fatigue and recovery effects in the 931 tube mentioned by Cobine. The operation of the tube is, therefore, limited to fairly low noise currents, and that only after some aging each time used.

~~SECRET~~

~~SECRET~~

as shown in Fig. 3, provision was made for noise source bandwidths of 150 kc/sec and 475 kc/sec. In the latter two cases shunt-peaked coupling was used.

The noise power output from the noise source was measured with an American Thermo-Electric Co. Type 93-L thermocouple designed for applications to and beyond 20 Mc/sec, used as a voltmeter by adding 10000 ohms in series. The thermocurrent was measured with a low resistance F. W. Paul Company microammeter. The entire meter was calibrated with d-c obtained from batteries. This calibration is shown in Fig. 9. Furthermore, the meter was checked against the General Radio vacuum tube voltmeter for frequency sensitivity. It maintains its reading to $\pm 5\%$ up to frequencies of 20 Mc/sec.

- (2) The jamming r-f carrier was produced by a klystron oscillator. Careful observation on a good spectrum analyzer showed that the CW was free from incidental FM to considerably less than 0.1 Mc/sec. Attempts to modulate this by noise on the reflector were not favorable; pure AM could not be obtained. Similarly cathode modulation was not free enough from FM to constitute a clean-cut experiment. Thus the expedient was adopted of driving a double-cavity klystron amplifier from the oscillator and modulating the beam current of the amplifier by introducing the external noise on the amplifier grid with a-c coupling through a low capacity cable from the noise source. There was thus virtually no coupling back on the oscillator.

No difficulties due to attenuation of higher frequencies of the modulation should be experienced because of the finite Q of the cavities (usually of the order of 200) until the modulating frequencies exceed about 7.5 Mc/sec. Reaction of the beam current on the cavity is not expected to become important until higher frequencies are used.

The static curve of output power from the oscillator-amplifier as a function of the amplifier grid voltage is shown in Fig. 4. The grid was normally biased at zero volts, and thus a reasonably linear region was available for about 3 volts on each side. Tests with a sine wave oscillator showed the modulation characteristic depicted in Fig. 5. It took 6 volts rms to produce 100% modulation. The modulation index was measured with a circuit which was a modification of the conventional one (10).

- (3) The artificial radar signal was produced by a "pulsed-cavity" McNally tube, carefully designed and constructed by R. R. Nelson. The f-m distortion was kept relatively low to that produced by most pulsed reflector signal generators of that time and, in fact, provided stable operation essentially free from FM for pulses from 0.1 - 5 μ sec in length and at repetition rates of 500, 1000, and 2000 per second.
- (4) All attenuators used were of the "wave-guide beyond cut-off" type, designed by S. G. Sydorak. Each was calibrated against a standard attenuator in standard fashion.
- (5) The receiver itself was of an unconventional type, built by J. Ferry. It is of the variable bandwidth multiple double-tuned circuit narrowing in the widest band one single stage narrowing but of the double-tuned variety in the others. The available i-f bandwidths (at a crystal current of 0.35 ma) were 13, 3.2, 1.16, 0.37, and 0.12 Mc/sec. Fig. 6 shows the band-pass characteristics. Fig. 7 shows the response law; it is quite linear except at the extremes. The receiver showed very little, if any, regeneration when tested for this. In Table I are shown theoretical and experimental time of rise of a step-function, a good check on the band-pass characteristic*.

TABLE I Comparison of time of rise

I-f bandwidth	Rise time (theoretical)	Rise time (experimental)
0.12 Mc/sec	5.8 μ sec	5.5 μ sec
0.37	1.9	2.9
1.16	0.61	0.64
3.2	0.22	0.24
13.0	0.064	0.10 (video bandwidth limiting)

The i-f narrowing sections were inserted by means of a low-capacity rotary switch, except for the two narrowest which were complete separate plug-in sections.

The voltage output across a reactor in the second detector circuit (steady component) was brought out to a terminal and was used for measurement and monitoring purposes. In the experiments to be reported the gain was almost invariably set so that 0.5 - 1.0 volts was produced at this terminal.

* The time of rise of a step function taken between the 10% or 90% points should be closely equal to $0.2/f$ bandwidth.

~~SECRET~~

The video section of the receiver had a bandwidth of about 3.5 Mc/sec. See Fig. 8. The video output was fed by low capacity coupling into a P4 oscilloscope, somewhat altered to provide more stable operation. The oscilloscope tube was a 5L4. The sweeps of the synchroscope were calibrated with a damped sine wave oscillator of known frequency. The phase of the trigger to the pulsed signal generator relative to that initiating the sweeps was controlled by a device mentioned below.

B Procedure.

It was felt essential that all input power levels reported in this work should be measured relative to some fixed physical standard. The noise power output of the mixer and first stage of a receiver at a fixed crystal current in the absence of an input signal is an excellent and useful reference level. Thus all input powers were referred to the equivalent receiver noise power after 1 Mc/sec narrowing but still in the i-f. This was done as follows:

An unmodulated c-w source was fed through its calibrated attenuator into the 13 Mc/sec receiver. (During this time the radar pulse was absent). With, say, 100 db attenuation negligible CW appeared at the second detector to be rectified. This detector is linear (see Fig. 7). The receiver gain was adjusted until the rectified receiver noise voltage at the second detector read some fiducial d-c value. Thereupon the attenuation was reduced until the voltage at the second detector was increased by a factor not far different from 1.414. Then, for that attenuator reading the c-w power at the receiver input terminals is just equal to the noise power. For let P_{CW} be the c-w power and P_n be the receiver noise power. It is well known that the addition of random variables occurs in power not voltage, and the CW and receiver noise are certainly random in phase. Thus the total power in the i-f circuit is

$$P = P_{CW} + P_n$$

but the rms voltage there is

$$V = (P_{CW} + P_n)^{1/2}$$

In the absence of CW,

$$V_C = (P_n)^{1/2}$$

Thus
$$\frac{V}{V_C} = \left(\frac{P_{CW} + P_n}{P_n} \right)^{1/2} = \left(1 + \frac{P_{CW}}{P_n} \right)^{1/2}$$

* This assumes a linear i-f section in the receiver and that the measurement of input power and noise takes place at the same point in the i-f section.

~~SECRET~~

Since the factor of 1.414 is obvious when $P_{CW} = P_N$. This factor would be retained in the detector output also, were it not for the small correction factor r which comes about because of the small difference between the rms and average values of the probability distribution of signal plus noise. Thus the correct value is 1.45.

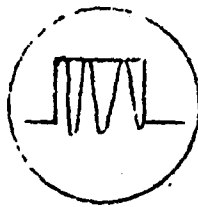
Thus far we have calibrated our jamming source in terms of 13 Mc/sec receiver noise, from which it is simple to refer it to a 1 Mc/sec receiver of the double-tuned single-narrowed type. It remains to show how the peak pulse power may be measured in the same units. The procedure originated in a suggestion by J. L. Lawson. If a c-w source is mixed with a pulsed r-f signal and fed into a receiver, there occur beats between the two sources during the pulse interval. The number of beats per unit time (i.e., the number of oscillations seen within the pulse) depends on the frequency difference between the two sources. If they are exactly attuned, there is a zero beat phenomenon, where, since the phases of the two are random, the CW sometimes adds to the pulse amplitude, sometimes subtracts. In fact the top of the pulse, instead of remaining stationary, simply moves up and down in more-or-less random fashion. The amplitude of the excursion depends on the relative strengths of the two sources.

The measurement then proceeds thus: The auxiliary c-w source shown in Fig. 1 (which may indeed be the jamming carrier itself) is fed through an attenuator along with the pulse through its attenuator into the receiver. The c-w attenuator is then calibrated in terms of noise power as described two paragraphs above. The c-w power is then increased until it is, say, $P_N + 20.0$ db. The gain of the receiver is reduced until little or no noise is apparent on the type A oscilloscope. Then the pulse attenuation is decreased until the beats have reasonable amplitude. The pulsed oscillator is then tuned to zero beat and its amplitude adjusted until the beats just come down to the base line. At first sight it might seem that, in this situation, the amplitude of the CW just equals that of the pulse, but this is indeed a pitfall. The c-w power has increased the d-c voltage output at the same time as well and the base line against which the measurements are made has moved up. Let the displacement of the base line be a . This then is the voltage developed by the c-w source. Let the pulse height in the absence of CW be b . Then the pulse amplitude in the experiment beats between $b + a$ and $b - a$. Nominally we would set $b - a = 0$ in the condition described, but, by the argument above we must set $b - a = a$ or

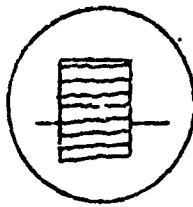
$$b = 2a$$

~~SECRET~~

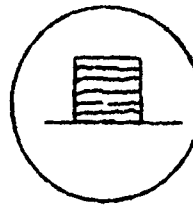
~~SECRET~~



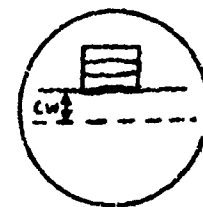
CW and pulse
off-tune



CW and pulse
in-tune



Appearance
for fiducial
condition



Appearance if
d-c coupling were
used

Thus the pulse amplitude is twice that of the CW, and the power difference is 6 db. Hence in making the hypothetical determination above, we obtain

$$P_{\text{pulse}} = P_n + 20.0 + 6.0 \text{ db} = P_n + 26.0 \text{ db}$$

and thus all that is necessary is to note the pulsed signal generator's attenuator reading at this point and the calibration is secured. Hence all measured powers are expressed in terms of i-f noise power, and, it will be seen, this is a very useful datum level indeed. This calibration is actually rapid, and is made some six or eight times per run. (The procedure, however, is limited to receivers whose i-f bandwidths are greater than 2/? or so, to avoid the phase reversal difficulties at the start and stop of the pulse.)

It may be noted in passing that this measurement serves as a check on the amount of FM on the pulse. If one uses a wide band receiver for the calibration the pulse is quite square on top. However, if FM exists, the beats between the CW and pulse are curved, not straight as they are for a clean pulsed signal. This condition was always noted in experiments to be described. The method also afforded a ready means of noting whether the CW was exactly on pulse frequency and not the other sideband accepted by the receiver. (This information is had by detuning the local oscillator and noting whether or not beats are introduced.)

C Technique of Assembling Data

The method and technique of assembling data requires discussion. The signal levels we shall be interested in are mainly low, because we ultimately demand the minimum discernible signal. For small signals, of the order of receiver noise power or less, the signal is discerned not as a square pulse of small height but as a tiny increase or decrease of the noise itself over a small interval of range.

~~SECRET~~

706-11

~~SECRET~~

Experience has shown that the self-determined criterion for the signal threshold easily can vary by 4 db even for so-called skilled observers. This self-determined criterion was, in the past, found by slowly attenuating the signal until it was adjudged minimum discernible, or slowly increasing the signal to a similar condition. Individual psychological and physiological factors led to the spread of observations. Furthermore, there is no apparent systematic method of evaluating errors in each determination. It was suggested that the personal element may be eliminated, not entirely, but to a large extent, by obtaining statistical data in the following fashion

1° A set of 6 range positions, extending over 3 cm, were arbitrarily chosen and marked on the (5") oscilloscope face. A set of 6 push-buttons put the signal in at the selected range positions

2° The push buttons were incorporated in a timing circuit arranged so that depressing the button put the signal in for just 3 second, an arbitrarily chosen standard signal presentation time maintained through all experiments*, after which a relay automatically removed it from the field of observation

3° An attenuator was set at a prescribed level and the observer called or recorded the range position at which he felt the signal had appeared. In all he took 20 observations for each attenuator setting

4° The signal was decreased (or increased) 1 db and the procedure was repeated until it was sure that the observer had covered the range from where he correctly assigned the signal 100% of the time to where his guesses were purely random and uncorrelated.

5° From the number of correct assignments, in each set of 20 observations, is subtracted 1/5 the number of incorrect calls, for this represents the number of correct calls to be expected as a result of random guesses. The remaining number is expressed as a percentage of 20 and so recorded.**

The usual spread for a good observer, and also one who has taken some preliminary practice runs is about 4 db from 100% correlation to 0% correlation,

* Experiments have been performed by Lawson and his co-workers to investigate the dependence of signal threshold on signal presentation time

** The probability of n correct guesses in m trials, if each event is random, is given by the binomial distribution

$$P_n^m = \frac{m!}{n!(m-n)!} \left(\frac{1}{6}\right)^n \left(\frac{5}{6}\right)^{m-n}$$

~~SECRET~~

~~SECRET~~

extrapolated in each case. The practice, with scoring is absolutely necessary so that the observer may learn the distinguishing characteristics of exceedingly small signals.

From the curve of percent correlation vs attenuator setting (a typical example is shown in Fig. 11), the 50% correlation point is recorded as the arbitrarily defined minimum discernible signal or signal threshold. As stated, this is about 2 db smaller than the signal that can be seen 100% of the time. However, such a signal is still an exceedingly small increase in the wild gyrations of the noise.

The advantage of this method is that amongst trained observers the individual spreads are usually small, of the order of 1 db or less. The statistics of the method will be discussed in the forthcoming report of Lawson *et al.* One can state from it that the probable statistical spread in the results for 20 observations and 6 positions is 15% at 70% calculated correlation, 20% at 30% calculated correlation.

Generally speaking, on the grounds of reproducibility it is felt that the experimental results quoted in this report are accurate to about ± 1 db unless otherwise stated. Residual systematic errors are extremely hard to evaluate, but, judging from repeatability and comparison, one feels that this figure is not seriously compromised. Accidental errors arise from (1) fatigue and faulty judgment effects in the observer, (2) fatigue effects in the noise source, (3) drifts in jammer frequency etc.

A typical data sheet is shown in Fig. 10.

IV EXPERIMENTAL RESULTS

With the experimental procedure and arrangement previously described, the following sets of parameters were varied and their effect on the signal threshold ascertained. For variation in pulse length, the values of 3, 1, 0.3, 0.1 μ sec were chosen; the i-f bandwidth was varied from 120 kc/sec to 13 Mc/sec in four steps; the intensity of the jamming carrier was varied to 31.2 db above the mean receiver i-f noise power in the 1 Mc/sec i-f bandwidth; the percent modulation* was varied from 0 to 70; the jamming noise source bandwidth, from 150 kc/sec to 5.5 Mc/sec. Although not all possible combinations of the above conditions were investigated (which would have led to something ponderous -- more than a thousand curves!) representative results were obtained in each case.

* Modulation percentage is defined in the following way. If a sine wave of peak amplitude V volts produces a given percent modulation (defined in the usual way), the modulation percentage for noise is stated to be that same value when the rms noise voltage is like that of V .

~~SECRET~~

A Effect of CW

Since in these experiments the noise sidebands are always accompanied by the c-w carrier, an investigation of the jamming efficiency of unmodulated CW was undertaken. The CW was in every case set exactly on the pulse mid-frequency and varied in intensity. In Fig 12 is plotted the signal threshold, S_t , in db above the receiver noise in the 1 Mc/sec bandwidth, vs. c-w power in db above the receiver noise in each respective i-f bandwidth, viz. the parameters on the curves. In the case of the three bandwidths examined about 3 db loss in S_t ensues for large amounts of jamming power. For the 13 Mc/sec i-f case, the 3 db loss is reached at about 20 db of CW above noise; for the 1.0 Mc/sec i-f, at 10 db above noise; for the 0.12 Mc/sec i-f, at about 25 db above noise. This last curve apparently shows the effect of incipient saturation by the extra decrease of 3 db at 40 db of CW.

Thus, one sees that there is a sharp limit to the deleterious effects of c-w jamming provided no overloading ensues. This same conclusion has been reached in dependent experiments (not yet reported) by Lawson and Johnson of this group. A mathematical argument which tends to justify this conclusion will be presented in another report, although it must be urged that the most convincing reasons for the limit in effect are the experiments themselves.

For all bandwidths jamming starts in at about the same c-w power relative to the receiver noise power in each bandwidth and then increases to an asymptotic value. A study of the so-called "North" curves (see reference 4) leads one to expect just these results. The probability curves are altered by the presence of the CW by an amount depending on the ratio of CW to noise power. For large amounts of CW the probability curves are unaltered in shape, but merely shifted along the scale. Hence the ceiling on the deleterious effects of the CW is easily understood.

In the sequel the terms "10 db jamming" will be used to designate "the unmodulated jamming r-f carrier is 10 db above receiver noise in the 13 Mc/sec receiver". It is interesting to note that 10 db c-w jamming has caused the full 3 db loss at 1.0 Mc/sec i-f bandwidth, about 1 db at 13 Mc/sec and 3 db at 0.12 Mc/sec. By 20 db jamming, all bandwidths show a loss in S_t of 3 db.

The interpretation of the results to follow, then, will be largely uninfluenced by any arguments as to the effectiveness of the c-w terms for this is almost uniform in all bandwidths.

Some question as to whether a large CW term of random phase with respect to the pulse may or may not cause a sort of "coherent integration"⁽¹¹⁾ of the signal in the noise may be raised. Such integration, if it exists, should presumably alter the square root law of repetition rate dependence. To check this point, Fig. 12a has been prepared from data taken at a 1.6 Mc/sec 1-f bandwidth, 1 usec pulse, sweep speed of 1.2 mm/usec, video bandwidth of 10 Mc/sec. The repetition rate was varied from 50/sec to 3200/sec. It is clear that, within experimental uncertainty, the square root dependence of signal threshold on PRF does indeed hold, and hence no apparent "coherent integration" takes place.

B Jamming Effectiveness as a Function of 1-f Bandwidth and Pulse Length:

Figures 13 - 16 show the signal threshold (50% correlation points) for the five 1-f bandwidths investigated, for respectively, the four pulse lengths in question, and for (1) no jamming, (2) 10 db jamming, and (3) 20 db jamming. The other radar parameters are stated on the figures. A modulation index of 50% was employed in this and every other case, unless a statement to the contrary is explicitly made. In every case the 13 Mc/sec point was increased 0.5 db relative to the others to correct for the difference between the 3 db bandwidth and the noise bandwidth of a receiver when a double tuned circuit is multiply narrowed compared to when it is singly narrowed (See Appendix B)

From Fig. 13, for a pulse length of 1 usec, the optimum bandwidth in the absence of jamming is close to 1.25 Mc/sec. At this point S_t is 8 db below the receiver noise power on this bandwidth. The curve seems to approach the 45° asymptotes predicted from simple theory on each side of this optimum. With 10 db jamming the optimum bandwidth has moved slightly toward the wider region, and now S_t at optimum is about 1 db above noise. Thus there is a loss in radar effectiveness of 9 db. For 20 db jamming, the optimum has moved distinctly to the right and the signal threshold at optimum is 7 db above noise. The optimum bandwidth is about 1.5 Mc/sec. Although the curve is quite flat about the optimum, the curves for no jamming, 10 db jamming, and 20 db jamming are quite parallel below the optimum bandwidth, but show a sort of convergence at wide 1-f bandwidths. The significance of this will be discussed further on and in Section IV D.

Fig. 14 shows a similar set of curves for a 0.3 usec pulse. The optimum bandwidth for no jamming is about 3.6 Mc/sec or 1.1 x 1/pulse length. At optimum, S_t is about 7 db below receiver noise in this bandwidth. The curves

~~SECRET~~

for 10 db and 20 db jamming are closely parallel for bandwidths narrower than optimum, but again seem to converge for bandwidths above optimum. The optimum bandwidths for the jammed cases are about 5.5 Mc/sec and 6.2 Mc/sec respectively.

The 3 usec pulse results are shown in Fig. 15. The optimum bandwidth without jamming is 0.4 Mc/sec or $1.2 \times 1/\text{pulse length}$. The S_t at optimum is 6 db below noise. The optimum bandwidths for 10 db jamming and 20 db jamming are, respectively, 0.45 Mc/sec and 0.7 Mc/sec. The same relative convergence at wide bands is noticed. Furthermore, on an absolute power scale the longer pulse lengths give the expected smallest signal discernibility (the pulse energy is greater). The curves are roughly parallel for bandwidths below optimum.

Finally, the results for the 0.1 usec pulse are depicted (without too much confidence) in Fig. 15. The optimum bandwidth from the curve for no jamming is slightly above 10 Mc/sec, or just about the reciprocal of the pulse length. That the optimum bandwidths for jammed conditions are wider can be seen from the trend in the curves, although sufficiently wide bandwidths were not available to identify them precisely. The results for the 0.1 usec pulse are on somewhat weaker footing than the remaining data because of the difficulty of producing such a narrow pulse with a flat top and free from incidental FM, because of the effect of the video narrowing, and because of the difficulty of accurately measuring the pulse length. Furthermore, there is a "presentation loss" relative to the 1 usec pulse, due to the geometrical factor of narrow signal width. This will be discussed more fully in the forthcoming report by Lawson et al. However, despite these factors, the results are reasonably in accord with predictions; e.g., the slopes of all the curves (which are fairly parallel) approach 45° for narrow i-f bandwidths; the beginnings of a convergence at wide bandwidths can be seen. At optimum bandwidth, for no jamming the signal threshold is perhaps 4 db below noise; for 20 db jamming, it is perhaps 6 db above noise at this bandwidth, but this last is a questionable extrapolation.

An interesting comparison can be made between these results and those calculated from Haeff's formula: ⁽⁶⁾ viz .

$$S_t \sim B^{\frac{1}{2}} \left(1 + \frac{1}{B \tau} \right)$$

He obtains an optimum bandwidth of $1/\text{pulse length}$ in comparison with our figure of $1.2 - 1.3/\text{pulse length}$. If we assume Haeff's functional form with our factor of 1.3 in place of his 1, the unjammed curve slopes can be compared in the

~~SECRET~~

following table (the experimental values come from Fig 17)

TABLE II. Comparison of Haeff's formula with experimental values.

$\frac{B}{B}$ max	Sig. Power (Haeff)		Sig. Power (exp'tal)	
	Sig	Power min	Sig	Power min
0.1	5.1	db	5.0	db
0.3	1.9		2.0	
1	0	(adjusted)	0	
3	1.2		2.0	
10	4.6		5.8	

Thus the agreement is quite good

It is instructive to compare the signal threshold for the several cases discussed. Thus in Fig 17 has been plotted a universal curve embodying the results of Fig. 13 - 16. S_t has been plotted as a function of B/B , and some of the results are summarized in Table III

TABLE III Summary of numerical results.

Pulse Length	Jamming conditions			
	none	10 db	20 db	
3 μ sec	-9.8	-2.3	+0.2	Numbers refer to S_t at optimum bandwidth measured in db above receiver noise power in the 1 Mc/sec i-f bandwidth
1	-7.3	+1.7	+9.1	
0.3	-1.6	+5.7	+8.3	
0.1	+6.0	+12.2 (?)	+17.2 (?)	

Without a specific comparison we may say that the general shape of the curves in the absence of jamming follows the accepted behavior. While it is true that the signal-to-noise ratio at optimum bandwidth should be independent of pulse length (as can be seen from any dimensional and energy argument), scaled up these 'no jamming' curves do not quite agree, but nevertheless are not in great disagreement. The scaling argument is incomplete unless the sweep length is scaled likewise by the pulse length; this accounts for some of the spread of the points in Fig 17. In Table IV the values are corrected by this factor, obtained from the results of Lawson and his co-workers.

TABLE IV Comparison of signal threshold and pulse energy.

Pulse length	S_t at optimum bandwidth (corrected for presentation)	Pulse energy
3 μ sec	-10.8 db above noise in 1 Mc/sec bandwidth	-10.8 db (arbitrary level)
1	-7.3	-12.1
0.3	-3.6	-12.9
0.1	+2.8	-13.3

It can be seen that the minimum discernible pulse energy is not far from constant for all pulse lengths investigated.

The parallelism of the jamming curves at the narrower i-f bandwidths is to be expected. The jamming signal consists of a carrier plus noise sidebands; the assumption that they act as independent jammers seems reasonable. At narrow i-f bandwidths all ceiling effects due to clipping (see below) disappear, and the situation is largely as in the case of receiver noise alone*. (The effect of the c-w term has already been shown to be fairly small). The convergence of the jamming curves at wide bandwidths is likewise explained by the fact that here there is a fairly marked ceiling on the jamming noise and thus the jamming does not do as much harm as would be expected on a purely bandwidth-power basis. The fact that the receiver's own noise is most prominent at wide bandwidths adds but little to this effect at the jamming powers in question.

C. The Effect of Increase in Jamming Strength.

In Fig. 18 have been plotted sections through the curves of Fig. 13, for the bandwidths of 0.12 Mc/sec, 1.16 Mc/sec, and 13 Mc/sec, and hence the conditions therein enumerated hold here. (In addition were taken several intermediate points to fill in the large empty spaces in the curves). 1.16 Mc/sec is closely the optimum (unjammed) bandwidth, the other two, the very wide and very narrow cases respectively. While similar sections can be prepared from the curves in Figs. 13 - 16, if the need arises, Fig. 18 can be used to illustrate the general cases.

In the first place, all these curves should eventually approach a 45° slope; i.e., the signal threshold is proportional to the power in the jamming carrier. The curves presented show this tendency, although this theoretical slope has just about been attained at 20 db jamming. Thus S_t is not solely a linear function of the jamming carrier power, for small power levels. But this we know already from previous discussion. In addition to the c-w carrier and its noise sidebands we have receiver noise as well. For CW, S_t is a fairly complicated function of the jamming power, starting slowly and eventually sustaining a saturation increase of about 3 db for large jamming powers, somewhat in the form of a diode saturation

* It is tacitly assumed that any effect caused by the phase relationships between the two noise sidebands can be ignored.

~~SECRET~~

curve For noise sidebands alone, the efficacy of the jamming should be proportional to the jamming power; while the receiver noise is always with us. The combination of these processes leads to a curve which starts out flatter than the 45° slope and eventually approaches it. Heuristically, one can write the equation of the curves in the form

$$S_t = a + bJ$$

where J is the jamming carrier power and a and b (functions of m , among other things) are empirical constants to be taken from Fig. 18. The factor b is a measure of the effectiveness of the jamming noise. It should be small for the wide $i-f$ bandwidths (ceiling effect), larger for the narrower $i-f$ bandwidths. This is indeed the case. The factor a should be closely connected with the receiver noise power, but this is complicated by the $c-w$ term mentioned above. However, it should behave in similar fashion to the "no jamming" curves; this, too, is the case.

It seems, from the curves, that there is a slightly greater tendency for the narrower bandwidths (optimum and below) to reach their theoretical slope at lower jamming powers. This seems reasonable on two grounds: (1) the receiver noise is a larger fraction of the total noise at wide bands; and (2), on the basis of an analysis of the effects of clipping,⁽¹²⁾ the externally added noise becomes more truly random the narrower the bandwidth. That is, clipping makes the noise less effective.

As an example, if S_t and J are measured in units of noise power in a 13 Mc/sec wide receiver, the actual numerical values of a and b that give a reasonable fit to the curve for the 1.16 Mc/sec $i-f$ bandwidth are

$$a = 0.016 \text{ (in the same units)}$$

$$b = 0.008$$

Other pulse lengths and bandwidths behave in similar, if not identical fashion.

D. Effect of Modulation Index

Ideally, with sinusoidal modulation at 100% the power in the sidebands is just one-half the carrier power. However, when a more complex wave is used to modulate, this limit is exceeded. For example, one may easily convince himself that modulation by a square wave with mark equal to space leads to energy in the sidebands equal to that in the carrier. With noise of an extremely clipped type again we find equal power in the noise sidebands and in the carrier at 100% modulation (cf Van Vleet⁽¹³⁾). With completely unclipped noise, on the other hand we have many sharp peaks, some few of which rise to very great levels

~~SECRET~~

~~SECRET~~

so as to overmodulate the carrier, and many of which lie below the rms level and hence fail to produce full modulation. Thus, strictly speaking, 100% modulation can never occur with unclipped noise, for the accidental fluctuations would require a modulation characteristic of infinite extent between cut-off and saturation. In the case of a practical modulator, peaks of voltage greater than the reciprocal of the percent modulation times the rms voltage are clipped off. Thus there is a ceiling set on the patterns.

In Fig. 19 are shown curves for a 3 μ sec pulse; the S_t is plotted as a function of the i-f bandwidth for modulation percentages of 0, 18, 25, 50, and 70. The jamming noise bandwidth is 5.5 Mc/sec, the jamming level is 20 db. These curves all show, to the first order, analogous behavior with respect to the i-f bandwidth although, of course, the visibility is constantly reduced for greater modulation indices. There is, however, on careful inspection, a progressive shift of the optimum bandwidth to the right, indicating the oft-mentioned ceiling effect which reduces the effectiveness of the jamming noise at wide bandwidths. This tendency is brought out more clearly in Fig. 19c.

In this figure are shown sections through the previously mentioned curves of Fig. 19, taken at the three i-f bandwidths of 0.12, 1.16, and 13 Mc/sec respectively. In these curves the abscissa has been changed from m , the percentage modulation, to m^2 . The dashed curve was drawn in under the following consideration. Van Vleck⁽¹²⁾ has calculated the ratio of sideband energy to carrier energy as a function of the clipping level. He finds that as the rms noise level is indefinitely increased ($m^2 \rightarrow \infty$) the ratio of sideband to carrier energy in a practical device approaches unity. For 100% modulation on our definition, the ratio of sideband to carrier energy is close to 50%. As the noise modulation factor is reduced, there is less and less clipping (see Fig. 4), and it is stated in the source mentioned that all effects of clipping either on the spectrum or on the power distribution should be comparatively small once the modulation index is below 100%. Then below this figure one may well rely on the fact that the power in the noise sidebands is proportional to m^2 . Hence the dashed curve is a plot of the theoretical noise sideband energy distribution as a linear function of m^2 and this is expected to hold about up to $m^2 = 1$. The reference level for this curve is arbitrary, since we make the assumption that the signal threshold is proportional to the noise sideband power, ceteris paribus. But this supposition is distinctly wrong, for the S_t curves are flatter than the energy curve, and in fact the deviation of the curves from the theoretical may be taken as a measure of the loss in efficiency due to the clipping effects. Now the effects of clipping should become less serious as

~~SECRET~~

~~SECRET~~

the i-f bandwidth decreases, because all the Fourier components necessary to establish a solid ceiling are not added in. Thus, in the limit of narrow bandwidths there is every reason to suppose that the signal threshold curve should have the same shape as the energy curve. That is, the only thing of importance is the energy in the noise sidebands, since the noise now appears as random as receiver noise. This supposition is seen almost to be fulfilled in the case of the curve for the 0.12 Mc/sec i-f bandwidth. But there are distinct deviations in the other two cases (a small part due to the receiver noise itself). A more quantitative estimate of the ceiling effect will be made in connection with the next section.

E. Variation of Jamming Noise Bandwidth.

The jamming noise bandwidth is defined as the video bandwidth (to the 3 db down points) of the noise source overall to the driving point of the klystron amplifier. See Fig. 8. Since the noise source emits a spectrum flat to far greater frequencies than come in question here the amplifier and associated circuits do the essential limiting. Three different noise bandwidths were employed - by far the larger part of the data has been assembled with a noise bandwidth of 5.5 Mc/sec. However, noise bandwidths of 475 kc/sec and 150 kc/sec were used to investigate a 1 usec pulse over the entire i-f bandwidth range, for comparison with the 5.5 Mc/sec bandwidth. The results are shown in Figs. 20 and 21. Pulse length and other quantities (except jamming power) were not varied because it was felt that the behavior for this pulse length is representative; the signal threshold for other pulse lengths can be deduced from the arguments explaining this effect on a 1 usec pulse.

For 10 db jamming, the S_t for all three jamming noise bandwidths is virtually the same for the very wide i-f bandwidths. As the i-f bandwidth decreases, an optimum is shown, but for the narrower jamming noise bandwidths the optimum region is quite considerably flatter, compared with the 5.5 Mc/sec case. For the 475 kc/sec jamming noise bandwidth, the optimum IF is about 2 Mc/sec; for the 150 kc/sec noise bandwidth, the optimum IF is about the same. This is for 10 db jamming. For the 20 db jamming, the optimum are again, respectively, about 2 Mc/sec. The surprising thing, at first sight, is that there seems to be an optimum jamming noise bandwidth. The curve for the 150 kc/sec noise bandwidth

~~SECRET~~

~~SECRET~~

lies between that for the 475 kc/sec and 5.5 Mc/sec. At 1 Mc/sec i-f bandwidth, the increase in S_t for 10 db jamming is 2.7 db for the 475 kc/sec noise bandwidth, 1.5 db for the 150 kc/sec noise bandwidth over that for the 5.5 Mc/sec case. For 20 db jamming, the corresponding numbers are 1.5 db and 1 db respectively. For very narrow i-f bandwidth, the S_t curves show a slight tendency to lie in the order of decreasing noise bandwidths.

How are these results to be interpreted? One must bear in mind the following situation. In every case discussed the modulation index was 50%. Thus, since the rms noise voltage was set at this figure, all noise peaks of voltage greater than about twice rms fail to appear in the output. Thus there is clipping taking place at this figure, clipping which drives the r-f oscillator either out of oscillation or to saturation, depending on polarity. This results in a ceiling on the noise pattern and, in fact, the ceiling will be the more sharply delineated the more completely all the Fourier components are added up. Thus in the case of wideband IF the ceiling is clearly perceived, while the narrower the IF becomes the more the random character of the jamming noise is restored. For all the jamming noise bandwidths considered, the 13 Kc/sec i-f bandwidth may be considered fairly wide, and thus it is found that the signal threshold is the same for the three cases, for the jamming noise power in the IF is the same for the three cases.

As the i-f bandwidth is narrowed, the randomness to the noise pattern is restored in the order of 150 Kc/sec, 475 kc/sec and 5.5 Mc/sec. However, for very narrow bandwidths, the jamming noise power in the receiver increases directly as the reciprocal of the jamming noise bandwidth. This is so because all three cases were investigated at the same mean noise power. An experiment was performed and this conclusion was checked at the 120 kc/sec i-f bandwidth. Thus, the noise power increase is in the order of 150 kc/sec, 475 kc/sec, and 5.5 Mc/sec noise bandwidth. It thus is quite possible that there be some optimum jamming noise bandwidth. From these experiments it seems that the optimum is somewhere close to 0.5 Mc/sec noise bandwidth.

It is possible to assess the validity of this interpretation by an examination of the consistency between the experiments described in this section, and other experiments whose results likewise depend on clipping effects. Such experiments are those described in the previous section.

~~SECRET~~

~~SECRET~~

F. Clipping Factors.

Under normal conditions one would expect the curves of Fig. 20, for the VERY NARROW IF, to lie in the order of decreasing jamming noise bandwidth; in fact, separated by the ratios of the noise bandwidths. It is probably fair to say that the effect of clipping depends on m , the percent modulation, and α , twice the ratio of the jamming noise bandwidth to the i-f bandwidth. Three independent sets of data will be compared, viz., that from Figs. 13 - 15, that from Fig. 19a, and that from Fig. 20.

In Fig. 13 it is clear that the curves should fall uniformly if the jamming were unclipped. That they do not is due to the clipping factor. Let us examine the case of 30 db jamming; this is enough to indicate the behavior, and, moreover, the effect of the receiver noise power is comparatively small. We further assume that an i-f bandwidth of 120 kc/sec all clipping effects have disappeared. We then record the difference (in db) between the unjammed and 20 db jamming curves in column 3 of Table V. The clipping factor, F_c , as recorded in column 4, is the difference (in db) between the values in column 3 for an i-f bandwidth of 120 kc/sec and that for the bandwidth in question.

TABLE V. Clipping effects.

I-f BW	α	db diff.	F_c
0.12 Mc/sec	92	18.0	0 db
1.16	9.5	17.0	1 1 μ sec data
13.0	0.85	12.0	6
0.12	92	16.5	0
1.16	9.5	14	2.5 3 μ sec data
13.0	0.85	10.5	6
0.12	92	17.5	0
1.16	9.5	16.3	1.2 0.3 μ sec data
13.0	0.85	13.0	4.5

These three determinations of the relationship of F_c to α agree fairly well among themselves.

Now from Fig. 19a, we construct Fig. 1 below in the following way. It is felt that at 15% modulation, say, clipping effects should be negligible at all jamming noise bandwidths investigated. Thus the theoretical curve was fitted

~~SECRET~~

to the experimental ones at $m^2 = 0.25$. Then the discrepancy in db is plotted as ordinate in Fig. 1, m as abscissa. This is done for the same i-f bandwidth as in Table V. From the $m = 50\%$ section through these curves is constructed Table VI. The agreement between the two independent determination of F_c is tolerably good.

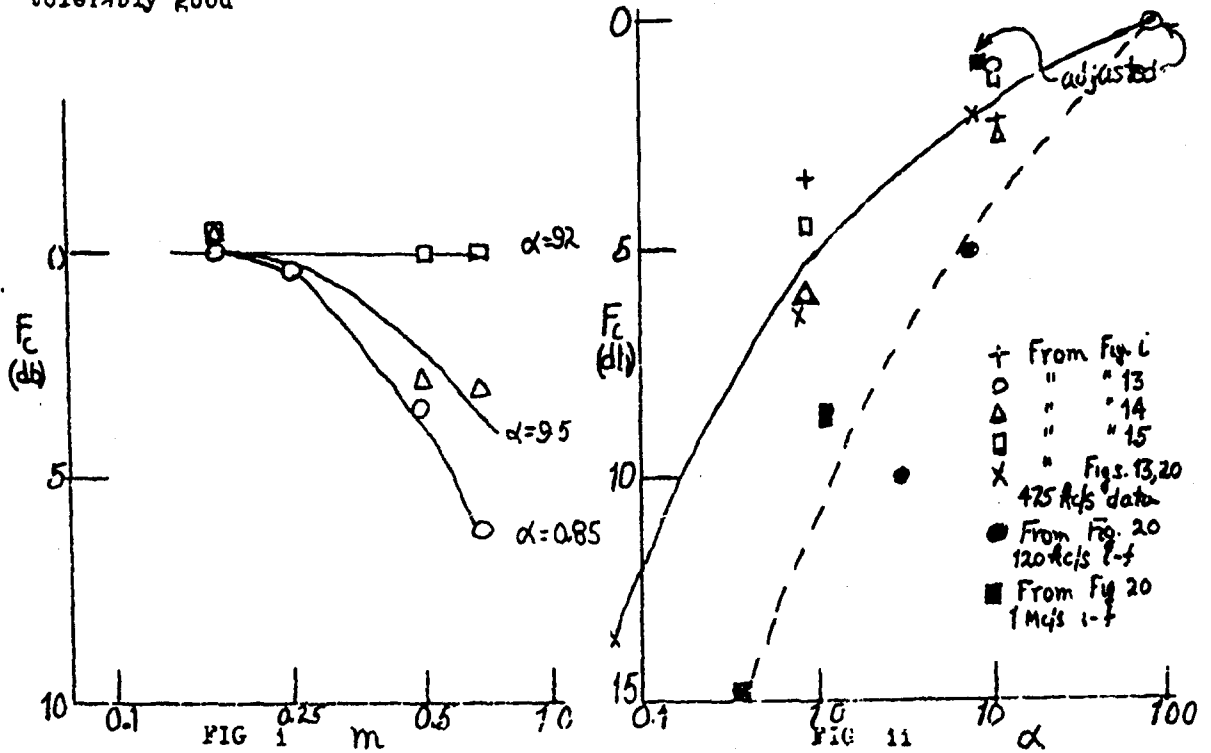


TABLE VI Clipping effects (continued)

I-f BW	α	F_c
0.12 Mc/sec	92	0.5 db
1.1C	95	2.3
13.0	0.85	4.0

but this agreement is in a certain sense disarming. For additional independent information on clipping effects comes from a study of Fig. 20 (together with the information on unclipped behavior in Fig. 13) and this study is in serious disagreement with the results immediately preceding. In Table VII are tabulated the values of F_c from a comparison of the 475 kc/sec curve of Fig. 20 (+20 db gain) with the unclipped curve of Fig. 13.

~~SECRET~~

TABLE VII Clipping effects (continued)

I-f BW	α	Jamming effect	F_c
0.12 Mc/sec	7.9	23.7 db	2 db (adjusted)
1.16	0.82	19.2	6.5
13.0	0.073	12.0	13.7

Column 3 gives the difference (in db) between the jammed and unjammed cases. If we accept the clipping factor of about 2 db for α of 7.9 (from Table VI), we can then fill in column 4 by this adjustment.

In Fig. 11 have been plotted all the data in Tables V, VI, and VII. In addition, from Fig. 20 there are also plotted the data taken at i-f bandwidths of 120 kc/sec and 1 Mc/sec; the clipping factors were obtained by a comparison of the actual S_t with that to be expected if all the jamming power were effective. At an α of 100 it is assumed that $F_c = 0$ db.

It is clear that not all of the data are consistent. That from Figs. 20 and 19a certainly agree, also that for the 475 kc/sec noise bandwidth case. However, a discrepancy of some 6 db or so at small values of α is apparent between these results and the others. No resolution of this paradox has been found: measurements of jamming noise power output directly confirm the expected result; no regeneration in the receiver has been discovered; curves of discrepancy vs m^2 for different jamming noise bandwidths, but the same α agree; no obvious experimental difficulty has been ascertained. One is led to the conclusion that some unsuspected source of experimental difficulty is being met, for it is not reasonable that the jamming effectiveness should depend on the noise bandwidth in any other way than already considered.

G Signal Threshold vs. Jamming Power

For the sake of comparison, sections through the curves of Fig. 20 (together with some additional points) are shown in Fig. 21. These are taken at i-f bandwidths of 0.12 Mc/sec, 1.16 Mc/sec. There is virtually nothing to add to the discussion already presented for the similar curves of Fig. 18.

H Signal Threshold Dependence on Pulse Lengths

In Fig. 11b are plotted some data taken from Figs. 13 - 16. S_t is plotted as a function of pulse length for different i-f bandwidths, for the case of no

~~SECRET~~

~~SECRET~~

Jamming and for 10 db jamming. The behavior is as expected and needs little comment other than to note that the curves are about the same shape, with and without jamming. Other things being equal, at any i-f bandwidth increasing the pulse length is an aid to radar range and an anti-jamming measure for the type of jamming under consideration. The narrower the IF, the more the aid obtained; the more the energy in the pulse, the better its visibility. However, one must be reminded that there is also some gain in discernibility ascribed to a "presentation gain" on the screen.

I. Restrictions on Results.

All the foregoing results apply to a linear detector, a linear type A oscilloscope display. There seems little reason to expect any significant difference, if the law of the detector or of the video-oscilloscope combination is changed. Any change in the law achieves the same results as could be obtained by the use of magnifying spectacles on the part of the observer, as Lawson has pointed out. Thus, in the genuine discernible region, where we have to deal with small signals and where presentation loss is not a serious question, the results should be uninfluenced by the deviation of the law from linearity.

Furthermore, the studies have not been carried to what may be called "high" jamming powers. The limits of power investigated are clear from the legends on curves. Nor have "off-frequency" jamming studies been undertaken.

V SUMMARY OF RESULTS AND CONCLUSIONS

In the preceding chapter have been discussed the experimental results and their interpretation. It is the intention here to apply these results to an estimate of the general vulnerability and/or invulnerability of radar sets to noise AM jamming, to point out what, if any, anti-jamming measures may be taken, to minimize the interference, to summarize the data in more readily usable form.

A. Anti-jamming Measures.

All AJ measures that prevent the jamming from entering the receiver are clearly desirable. Examples of such measures are: radar frequency shifts, good antenna pattern, polarization control, etc. However, once the jamming enters the receiver system little can be done to alleviate its effects. In general a

~~SECRET~~

somewhat wider i f bandwidth than is commonly used for the particular radar pulse is desirable, although the benefit to be obtained by this procedure is really quite negligible (perhaps 0.5 db). It should be reiterated here that radar set design considerations leading to better radar performance in general lead to better performance in the presence of jamming of the type studied here. Examples of this are indicated in the following table.

TABLE VIII Design considerations with regard to jamming

Design consideration	Effect on radar performance	Effect on performance against (wideband) jamming
Antenna gain, G	G^2	G
Peak power, P	P	P*
Pulse length, L	L	L
PRF	(PRF) ²	(PRF) ²

B Quantitative Estimate of Jamming Power

Little will be said on this matter for the reason that each tactical problem requires its own solution. Furthermore, values of S_t which one could have obtained from calculations based on reasonable guesses are almost as useful as the actual experimental results. Namely for the 13 Mc/sec IF, with 20 db jamming at 70% modulation the power in the jamming noise sidebands is about 14 db above the receiver noise at this i f bandwidth. Thus one would expect roughly a decrease in visibility of 14 db due to the noise about 3 db due to the carrier making 17 db in all. Actually from Figs 15 and 19 about 11.5 db is observed. The difference is largely due to clipping. Thus the discrepancy in the values is less than one order of magnitude. Where the jamming noise is again random as in the 0.12 Mc/sec i-f bandwidth, the calculated and experimental values practically agree (19.5 db vs 19 db). Furthermore a priori reasoning would indicate only a slight change in the optimum i f bandwidth, just as is found in the jamming experiments.

Thus calculations of the jamming power required to do a given job will not be seriously in error if one simply calculates the noise power at the receiver terminals and compares it with the receiver noise figure. The general method of calculation would follow the line adopted by Lawson⁽¹³⁾

However a more consistent procedure would be as follows:

* This is not true of course if the jammer scales his bandwidth by the same factor.

~~SECRET~~

- (1) Calculate the total jamming noise sideband power falling to the receiver i-f bandwidth in comparison with receiver noise. Let this ratio be J/N . This calculation is made from a knowledge of the jamming carrier power, its noise bandwidth, and the modulation index, m . Express this power ratio in db.
- (2) Add about 3-4 db to (1) to account for the carrier.
- (3) Correct for the clipping factor, F_c , according to m and α . This correction is indicated in the chart of Fig 22. F_c is given in db to be subtracted from (2) above.
- (4) This final answer represents the increase in signal power, expressed in db over that in the unjammed case, necessary for visibility in the presence of the jamming under consideration.

For example -- what is the loss in signal visibility under the following conditions:

Jammer carrier = 50 db above receiver noise.

Jammer video BW = 6 Mc/sec.

Jammer % modulation = 70.

Radar receiver i-f BW = 2 Mc/sec; $\alpha = 6$.

Pulse length = 1 μ sec.

- (1) Noise power in receiver. At 70% modulation, the sideband power is 6 db lower than the carrier power. (See p. 23). The receiver accepts 1/5 of this because of its bandwidth, i.e., -7.8 db. Therefore, the noise power in the receiver is

$$50 - 6 - 7.8 = 36.2 \text{ db over receiver noise.}$$

- (2) The carrier effect is 3 db.

$$36.2 \text{ db} \longrightarrow 39.2 \text{ db}$$

- (3) From Fig. 22 the clipping effect for $\alpha = 6$, $m = 70\%$ is about 4 db. Thus

$$39.2 \text{ db} \longrightarrow 35.2 \text{ db.}$$

- (4) Therefore the increase in S_t required by the jamming is 35 db.

C. Acknowledgement.

In conclusion it is a pleasure to acknowledge the aid of C. Harvey Palmer in taking some of the data, and the valuable advice and criticism of Dr. James L. Lawson during the course of this work.

~~SECRET~~

~~SECRET~~

REFERENCES

- (1) Sard, RRL Report 26.
- (2) Goudamit, RL Report 43-21.
- (3) Goudamit and Weiss, RL Report 43-20
- (4) North, Princeton Technical Report 6-C
- (5) Jordan, RL Report 61-23
- (6) Haeff, Navy Report 134
- (7) Taylor and Peterson, RRL Report.
- (8) Cobine, RRL Report 51
- (9) Cobine, RRL Report 55.
- (10) E. G. Terman, Radio Engineers' Handbook, p 989.
- (11) Emalie, RL Report 103-5/16/44
- (12) Van Vleck, RRL Report 57.
- (13) Lawson, RL Report 72-3/24/43

~~SECRET~~

~~SECRET~~

APPENDIX A SOME CONSIDERATIONS INVOLVED IN RADAR PERFORMANCE

Starred quantities (*) represent parameters varied in the course of present experiments

RF

- | | |
|--|--|
| 1° Power | 2° Noise figure |
| * a) Peak | a) Optimum operational characteristics |
| * b) Pulse length | d) Round-trip losses |
| c) Recurrence rate | 5° Local Oscillator |
| d) Pulse spectrum | a) Excess noise |
| 2° Antenna | b) Signal loss into LO coupler |
| a) Pattern | c) Frequency |
| 1) Gain as $G(\theta, \phi)$ | 6° Propagation Factors |
| 2) Polarization | a) Excess atmospheric noise |
| 3° Scanning | b) Refraction and focussing effects |
| a) Rate | c) Station and target locations |
| b) Type | 7° * Interference |
| 4° Plumbing | 8° Target reflection properties |
| a) TR recovery | a) Cross-section |
| b) R-f band-pass characteristics (including filters) | b) Fluctuations |
| c) Mixer | |
| 1) Law and type | |

IF AND VIDEO

- | | |
|---|--------------------------------|
| 1° Center frequency | 1) Peaking |
| 2° Frequency response | 2) Low frequency rejection |
| a) Amplitude and phase characteristic (type of bandwidth narrowing) | 3) Polarized narrowing |
| | 4) Etc |
| | c) Other video characteristics |
| 3° Law of 2nd detector | 1) Blanking |
| 4° Video | 2) Limiting |
| a) Amplification vs frequency | 3) Lengthening |
| b) Phase vs frequency (type of narrowing) | 4) Length discrimination |
| | 5) Etc |

~~SECRET~~

~~SECRET~~

PRESENTATION

- 1° Common types of presentation
 - a) A
 - b) B
 - c) PPI
 - d) RO
 - e) Expanded type
 - f) Etc.
 - 2° Type A oscilloscope
 - a) *Sweep rate
 - b) Intensity
 - 3° Noise height
- c) Focus
 - d) Type of screen
 - 1) Color
 - 2) Build-up and decay
 - 3) Grain size
 - 4) Dark or bright trace
 - e) Sweep length
 - f) Deflection-intensity laws

EXTERNAL FACTORS

- 1° Ambient light
 - 2° Physiological factors
 - 3° Observer
 - a) Inherent ability
 - 4° *Signal Presentation Time
- b) Training
 - c) Criterion for standard observer

~~SECRET~~

APPENDIX B

A single stage of a single-tuned circuit has a response curve (ideally) of the form $1/(1 + \omega^2)$; and so on. In this form, the 3 db bandwidth in each case is just equal to 2, and the higher the multiplicity of tuning, the closer the system function approaches the square form. The noise bandwidth (i-f) if defined as the equivalent rectangular band-pass characteristic, that gives the same noise power as the actual one. In the actual case, the noise power is given by

$$\int_{-\infty}^{\infty} \frac{d\omega}{1 + \omega^n}$$

where $n = 2, 4, 6, \text{ etc.}$ This is most easily integrated by changing variables from ω (real) to Z (complex) and integrating from $-\infty$ to $+\infty$ along the real Z axis, and closing the contour by a large semicircle in the positive half-plane. No contribution to the integral occurs on this half-circle of large Z , and there are only a finite number of simple poles in the positive half-plane. Thus the integral is simply given by $2\pi i \sum \frac{1}{n} R_p$, where R_p is the residue at a given pole. The results of some tedious algebraic summing give the following values: [if the circuits are multiply narrowed, we must evaluate integrals of the form

$$\int_{-\infty}^{\infty} \frac{dz}{(1 + z^n)^m}]$$

No. stages	Noise BW	3 db BW	difference	
1	3.14	2.000	1.95 db	singly-tuned
2	1.57	1.286	0.85	circuits
3	1.18	1.02	0.64	
4	0.985	0.868	0.55	
1	2.221	2.000	0.46	
2	1.67	1.604	0.2	circuits
1	2.096	2.000	0.2	triply-tuned
				circuits
1	2.038	2.000	0.08	quadruply-tuned
				circuits
1	2.020	2.000	0.04	quintuply-tuned
				circuits

~~SECRET~~

Thus in multiple double-tuned stages, the 3 db bandwidth and the noise bandwidth are virtually the same, while a single double-tuned stage differs in the two by about 0.5 db

A. M. Stone
February, 1945

~~SECRET~~

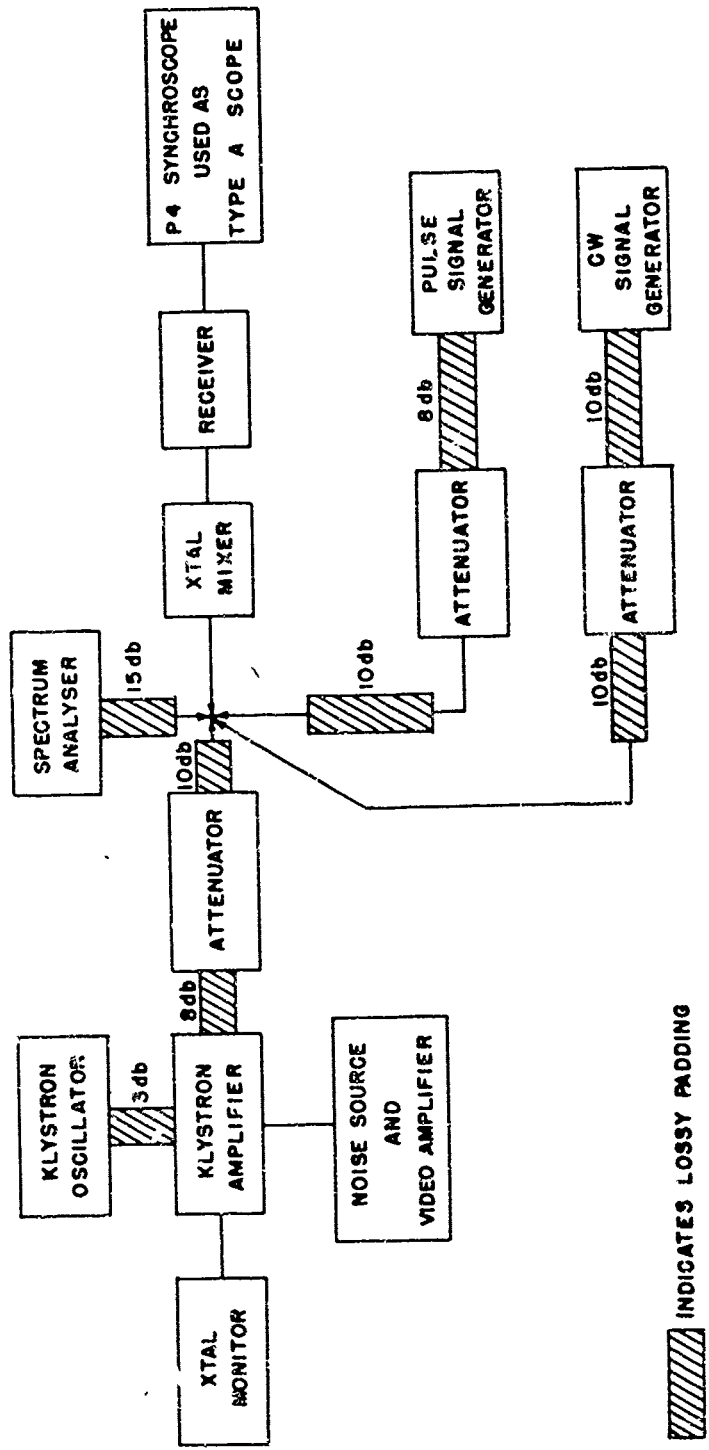


FIG. 1 BLOCK DIAGRAM OF EXPERIMENTAL APPARATUS

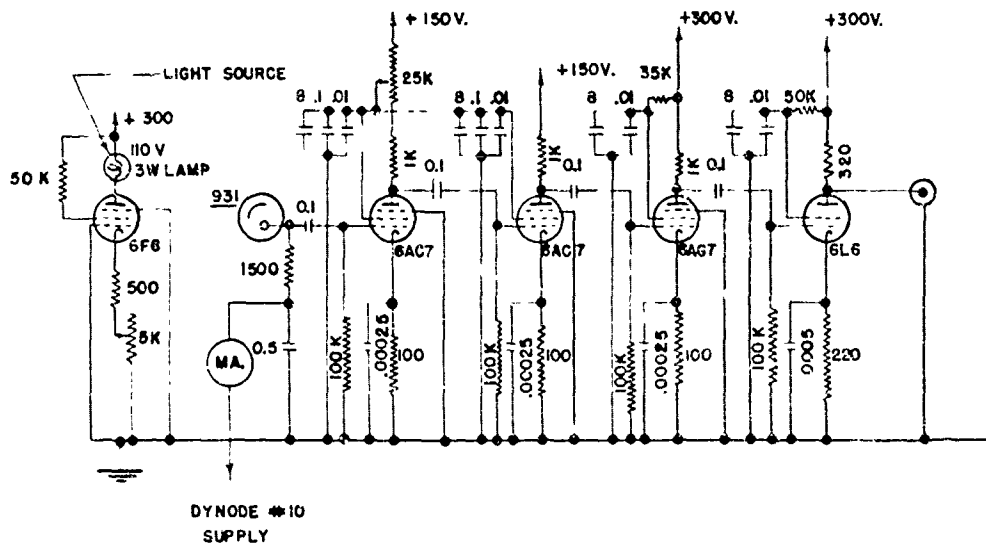


FIG. 2a NOISE SOURCE AND VIDEO AMPLIFIER

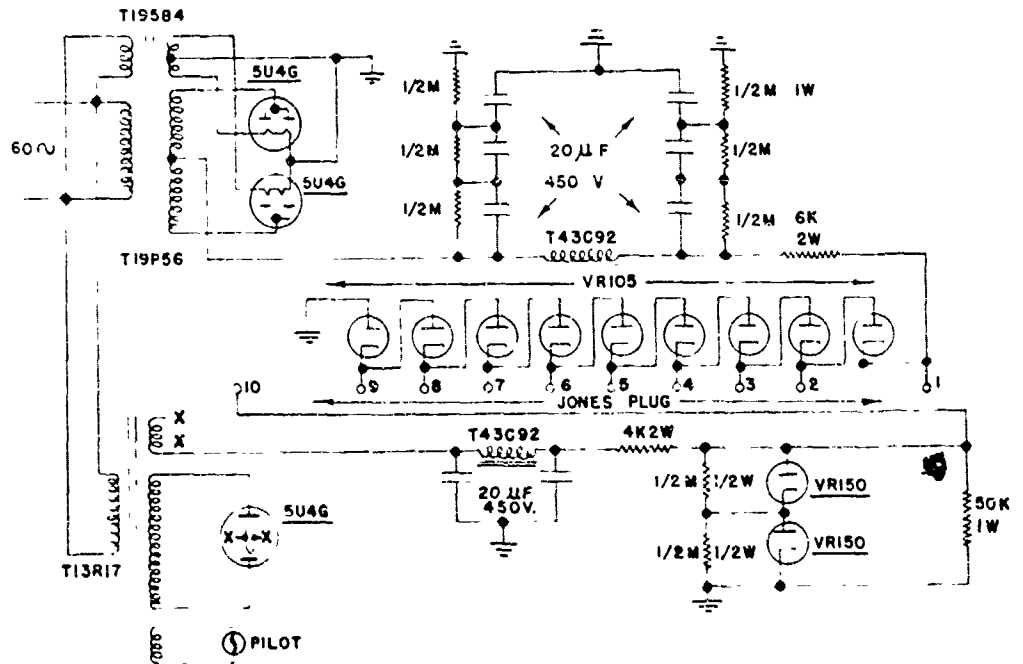
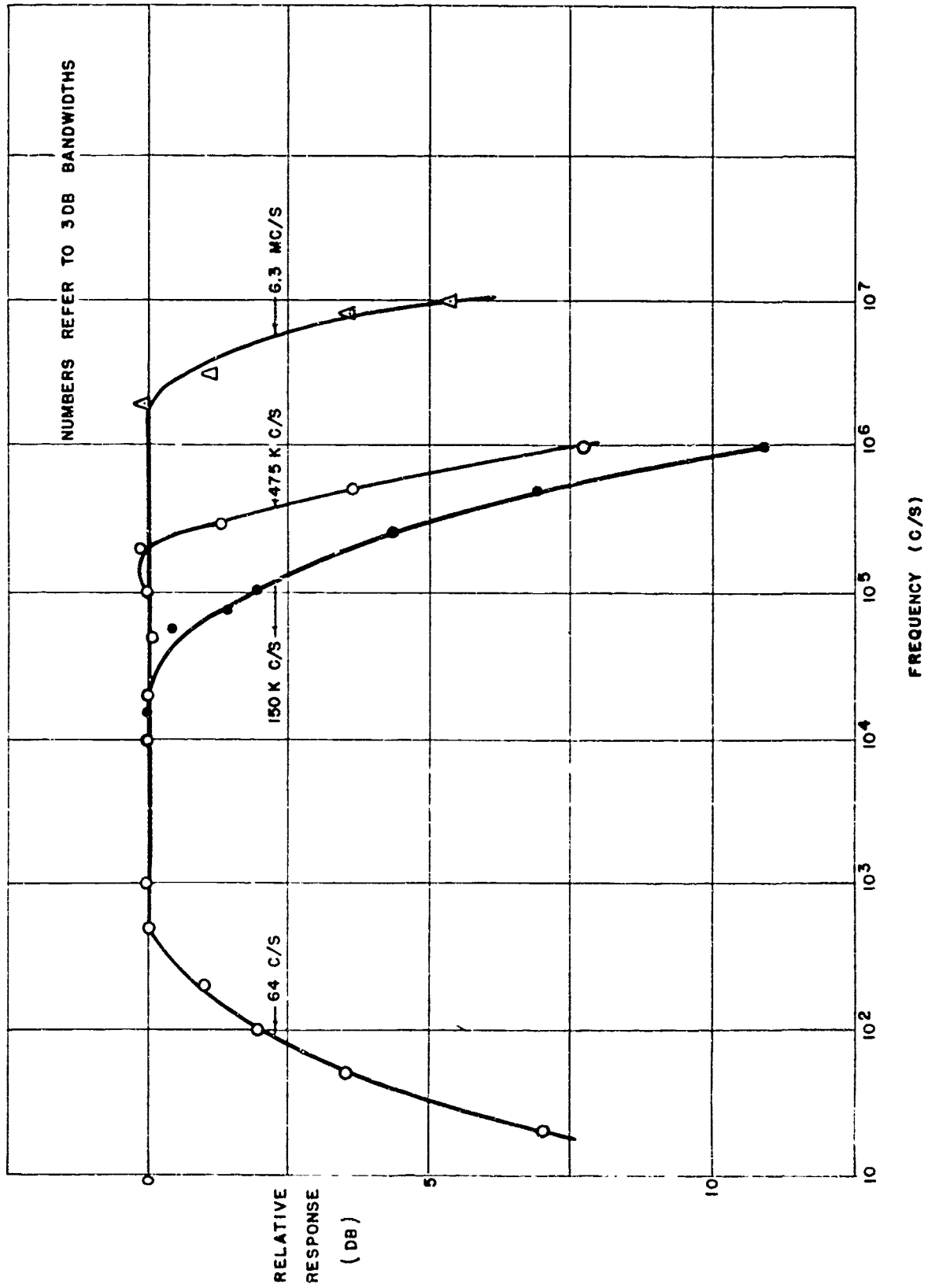


FIG. 2b POWER SUPPLY FOR 931 NOISE SOURCE



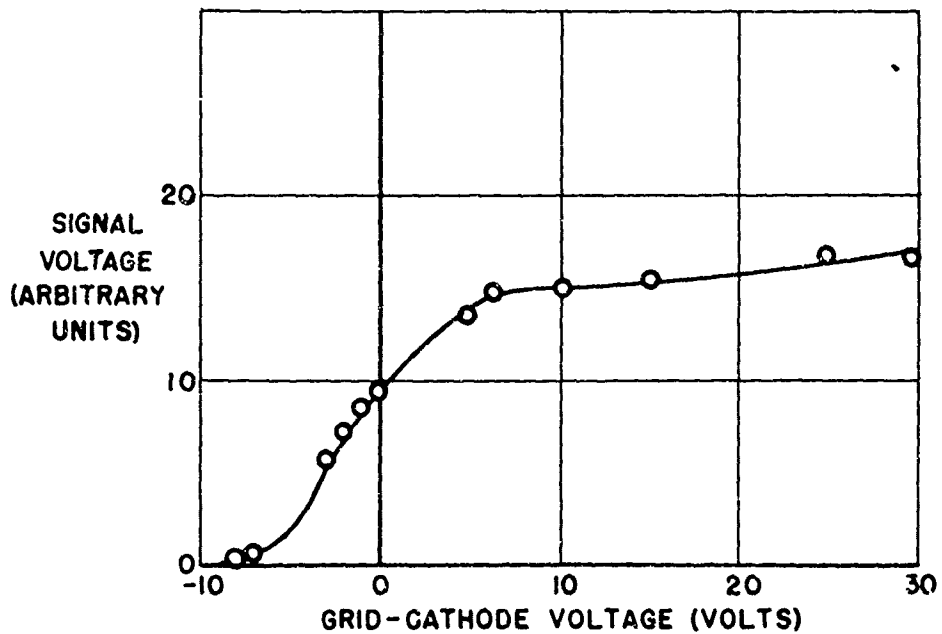


FIG. 4 KLYSTRON AMPLIFIER STATIC CHARACTERISTIC

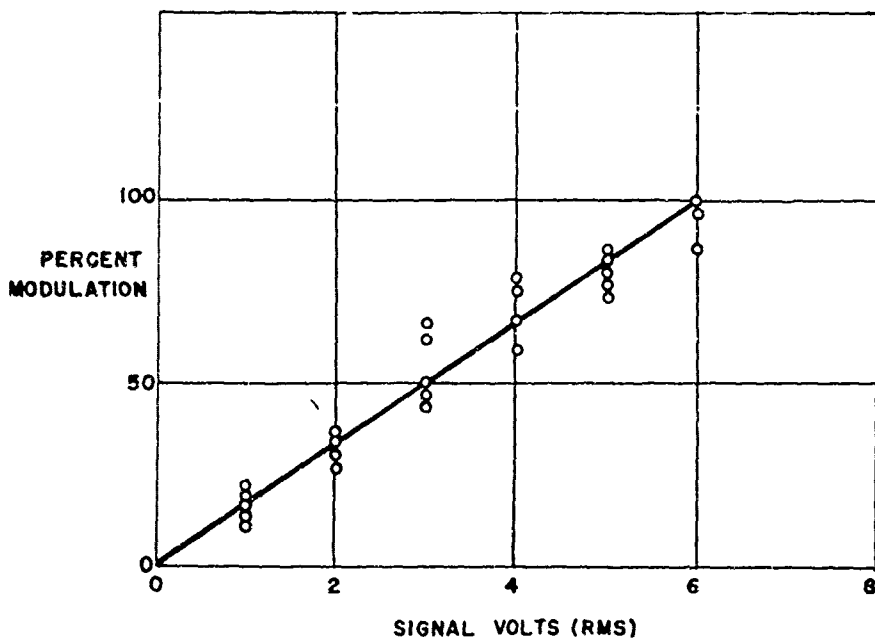


FIG. 5 MODULATION CHARACTERISTIC OF KLYSTRON AMPLIFIER

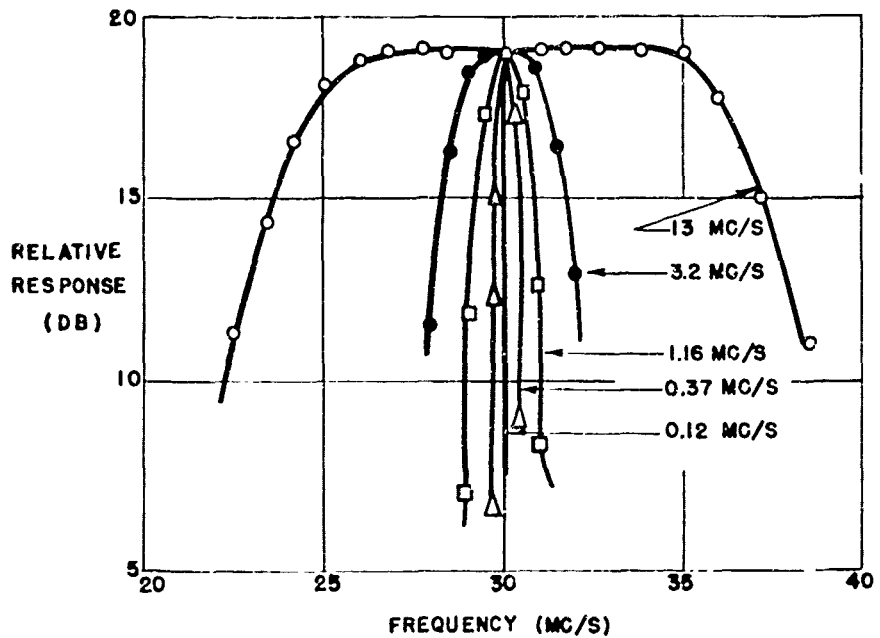


FIG. 6 RECEIVER I.F. ATTENUATION CHARACTERISTIC BANDWIDTHS ON CURVES ARE TO 3DB DOWN FROM THE MIDFREQUENCY POWER

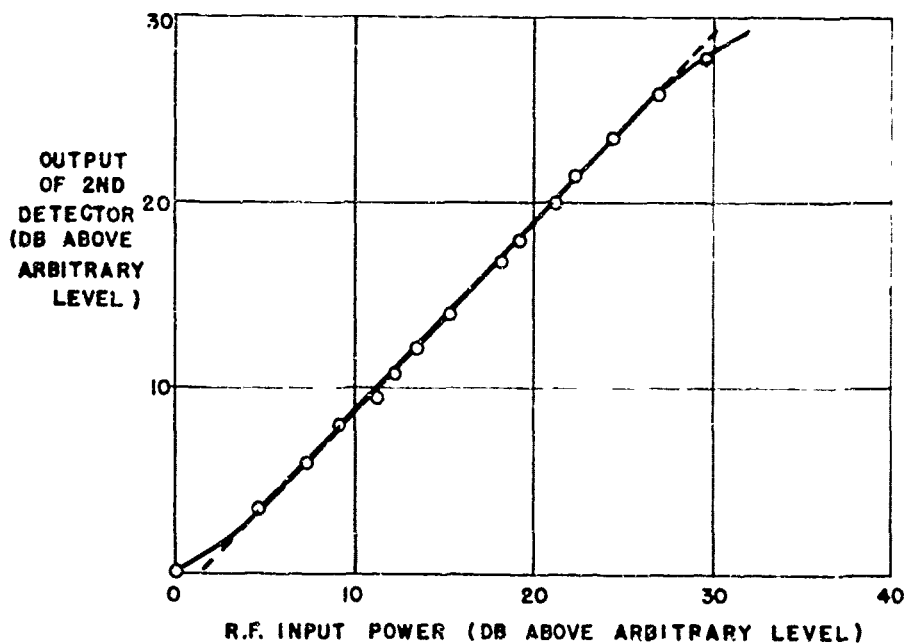


FIG. 7 OVERALL RECEIVER CHARACTERISTIC

~~SECRET~~

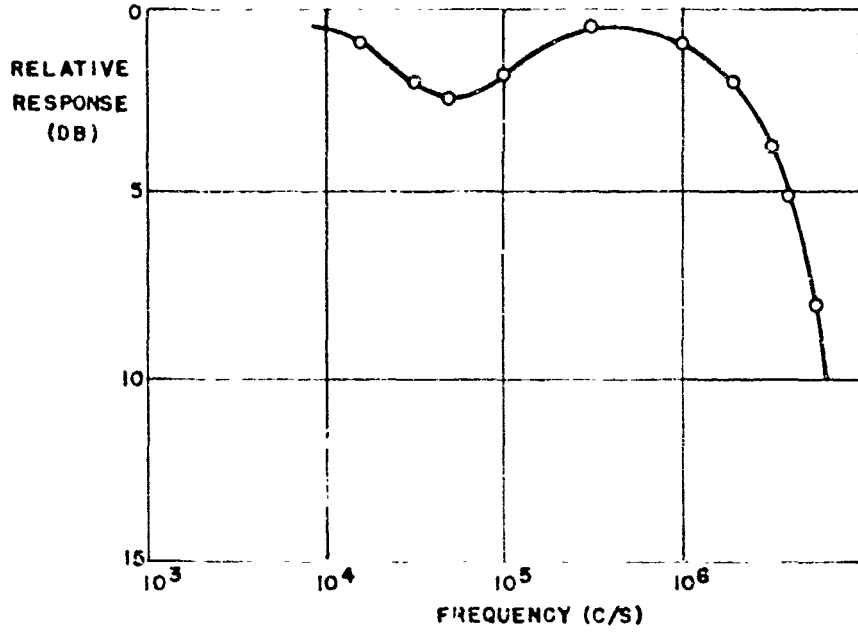


FIG. 8 RECEIVER VIDEO RESPONSE

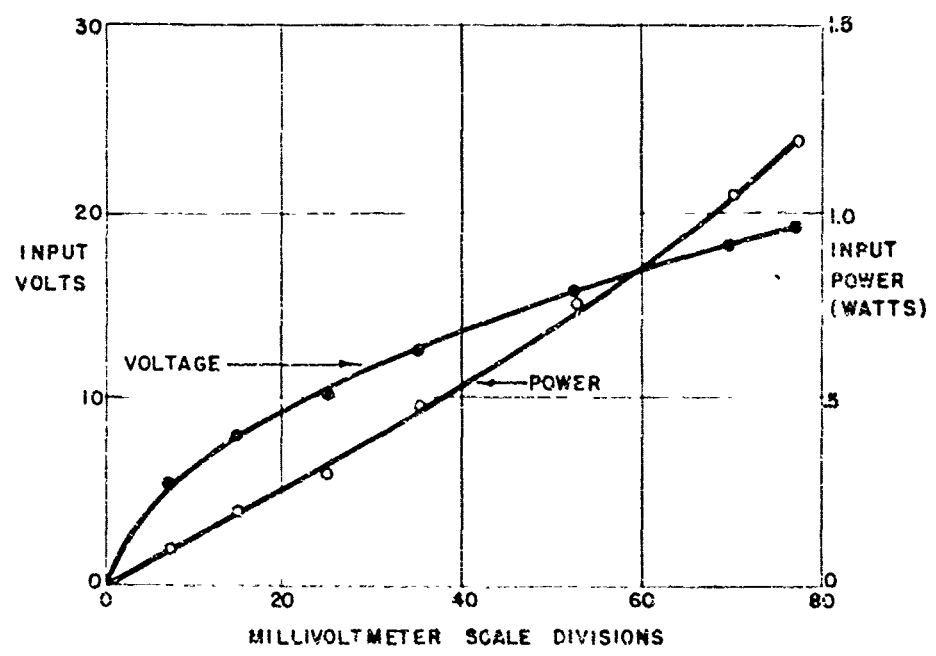


FIG. 9 CALIBRATION OF THERMOCOUPLE VOLTMETER

~~SECRET~~

~~SECRET~~

Date	10 22 51	CW = 1.4 x noise volt on 1.3 mc band	70.5
Operator	A. M. Stone	Jamming CW signal = 1.4 x noise	79.1
Waveform	1 cm	Signal = noise	71.0
Waveform	1000	For percent modulation	70
Repetition rate	10%	Crystal current	0.25 ma
Sample length	1000	Time per observation	3 sec
No. of runs per	6	Signal = noise after experiment	
Law of 2nd set	11000	Jamming signal = noise after exp	
Type of jamming	AM by noise	mm/sec - sweep speed	1.03
		Noise bandwidth	150 kc/sec

Jamming Signal	Band width													Atten rdg	No wrong	Corr %	50% rdg	dB		
10 dt	12	✓	✓	✓	✓	✓	✓	✓	✓	✓	✓	✓	✓	✓	✓	54	0	100	59.1 + 11 S = N 70	
		✓	✓	✓	✓	✓	✓	✓	✓	✓	✓	✓	✓	✓	✓	56	1	94		
		0	0	✓	✓	✓	✓	✓	✓	✓	✓	✓	✓	✓	✓	58	5	70		
		✓	✓	0	0	✓	✓	✓	✓	✓	✓	✓	✓	✓	✓	59	7	58		
		0	✓	0	0	✓	✓	✓	✓	✓	✓	✓	✓	✓	✓	60	11	34		
	✓	✓	0	0	0	✓	✓	✓	✓	✓	✓	✓	✓	✓	✓	61	15	10		
	3	✓	✓	✓	✓	✓	✓	✓	✓	✓	✓	✓	✓	✓	✓	60	0	100	66.5 + 4 S = N 71.2	
		✓	✓	✓	✓	✓	✓	✓	✓	✓	✓	✓	✓	✓	✓	63	1	94		
		✓	0	✓	✓	✓	✓	✓	✓	✓	✓	✓	✓	✓	✓	65	1	94		
		✓	✓	0	✓	✓	✓	✓	✓	✓	✓	✓	✓	✓	✓	66	5	70		
		✓	0	0	✓	✓	✓	✓	✓	✓	✓	✓	✓	✓	✓	67	11	34		
	1 16	✓	✓	✓	✓	✓	✓	✓	✓	✓	✓	✓	✓	✓	✓	66	0	100	71.5 + 0 S = N 70.6	
		✓	✓	✓	0	✓	✓	✓	✓	✓	✓	✓	✓	✓	✓	68	1	94		
		✓	✓	0	0	✓	✓	✓	✓	✓	✓	✓	✓	✓	✓	70	3	82		
		✓	0	✓	0	0	✓	✓	✓	✓	✓	✓	✓	✓	✓	72	10	40		
0		✓	0	0	0	✓	✓	✓	✓	✓	✓	✓	✓	✓	71	10	40			
3 2	0	✓	0	0	✓	✓	✓	✓	✓	✓	✓	✓	✓	✓	66	0	100	71.3 + 0 S = N 71.7		
	✓	0	✓	✓	✓	✓	✓	✓	✓	✓	✓	✓	✓	✓	69	2	88			
	✓	0	0	0	✓	✓	✓	✓	✓	✓	✓	✓	✓	✓	70	4	76			
	✓	0	0	0	0	✓	✓	✓	✓	✓	✓	✓	✓	✓	71	8	52			
	0	0	✓	0	0	0	✓	✓	✓	✓	✓	✓	✓	✓	72	11	34			
13	0	0	✓	0	0	✓	✓	✓	✓	✓	✓	✓	✓	✓	70	2	88	71.9 + 0 S = N 71.4		
	✓	✓	✓	✓	✓	✓	✓	✓	✓	✓	✓	✓	✓	✓	71	3	82			
	✓	0	✓	✓	✓	✓	✓	✓	✓	✓	✓	✓	✓	✓	72	9	46			
	0	0	✓	0	0	0	✓	✓	✓	✓	✓	✓	✓	✓	73	13	22			
	✓	✓	✓	✓	✓	✓	✓	✓	✓	✓	✓	✓	✓	✓	69	1	94			
✓	✓	✓	✓	✓	✓	✓	✓	✓	✓	✓	✓	✓	✓	68	0	100				

FIG 1) Typical data sheet

~~SECRET~~

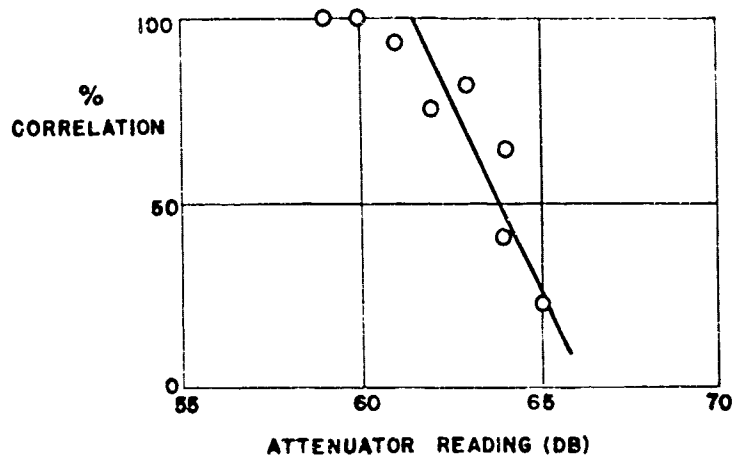


FIG. 11a SAMPLE CORRELATION PLOT

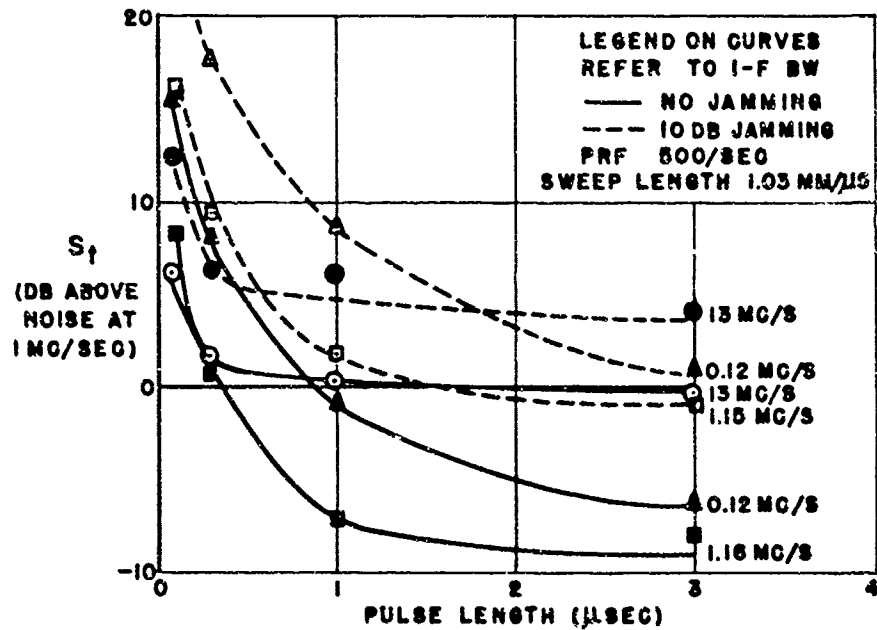


FIG. 11b SIGNAL THRESHOLD AS A FUNCTION OF PULSE LENGTH

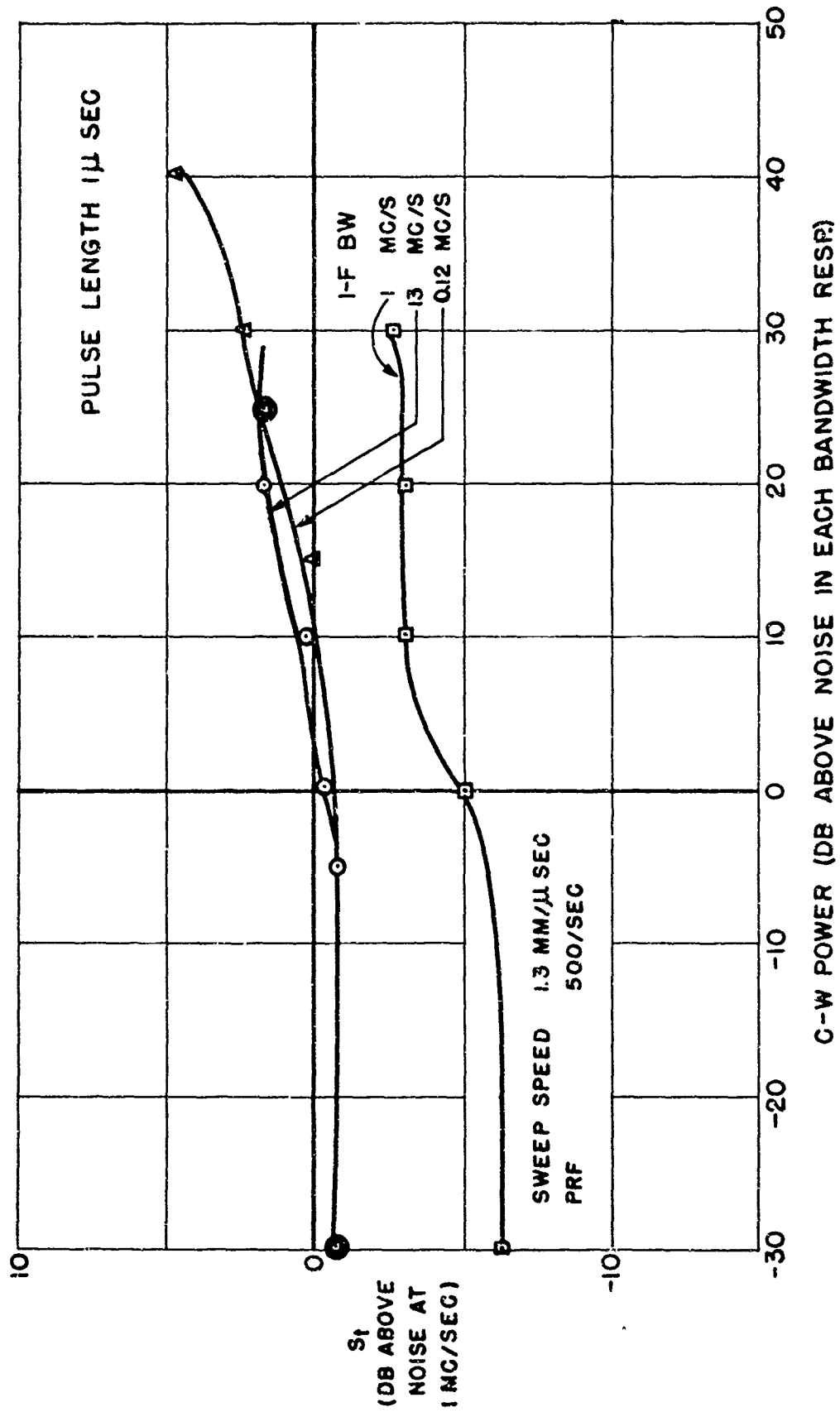


FIG. 12 JAMMING EFFECTIVENESS OF CW

~~SECRET~~

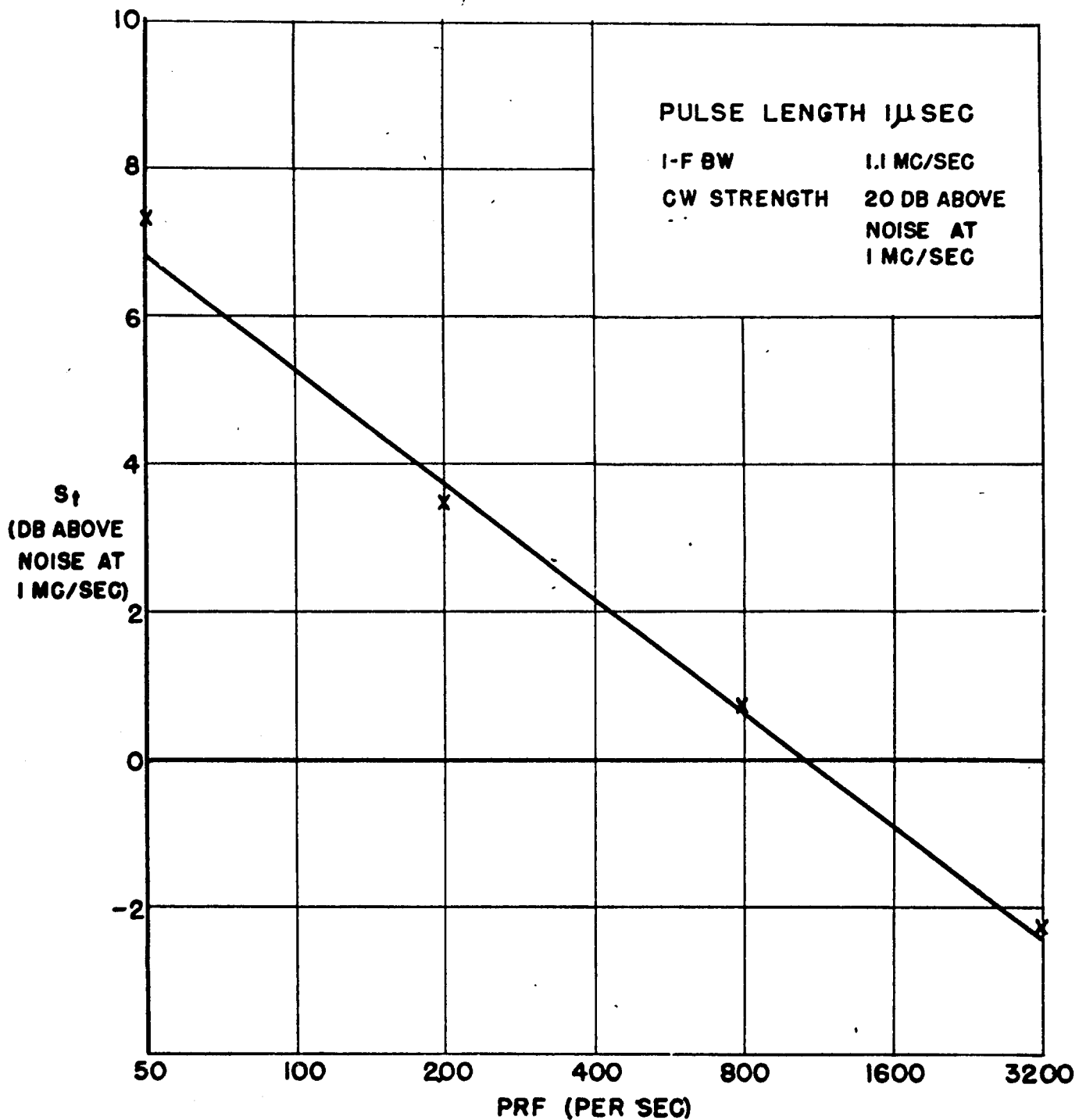


FIG. 12a SIGNAL THRESHOLD AS A FUNCTION OF PRF FOR CW JAMMING

~~SECRET~~

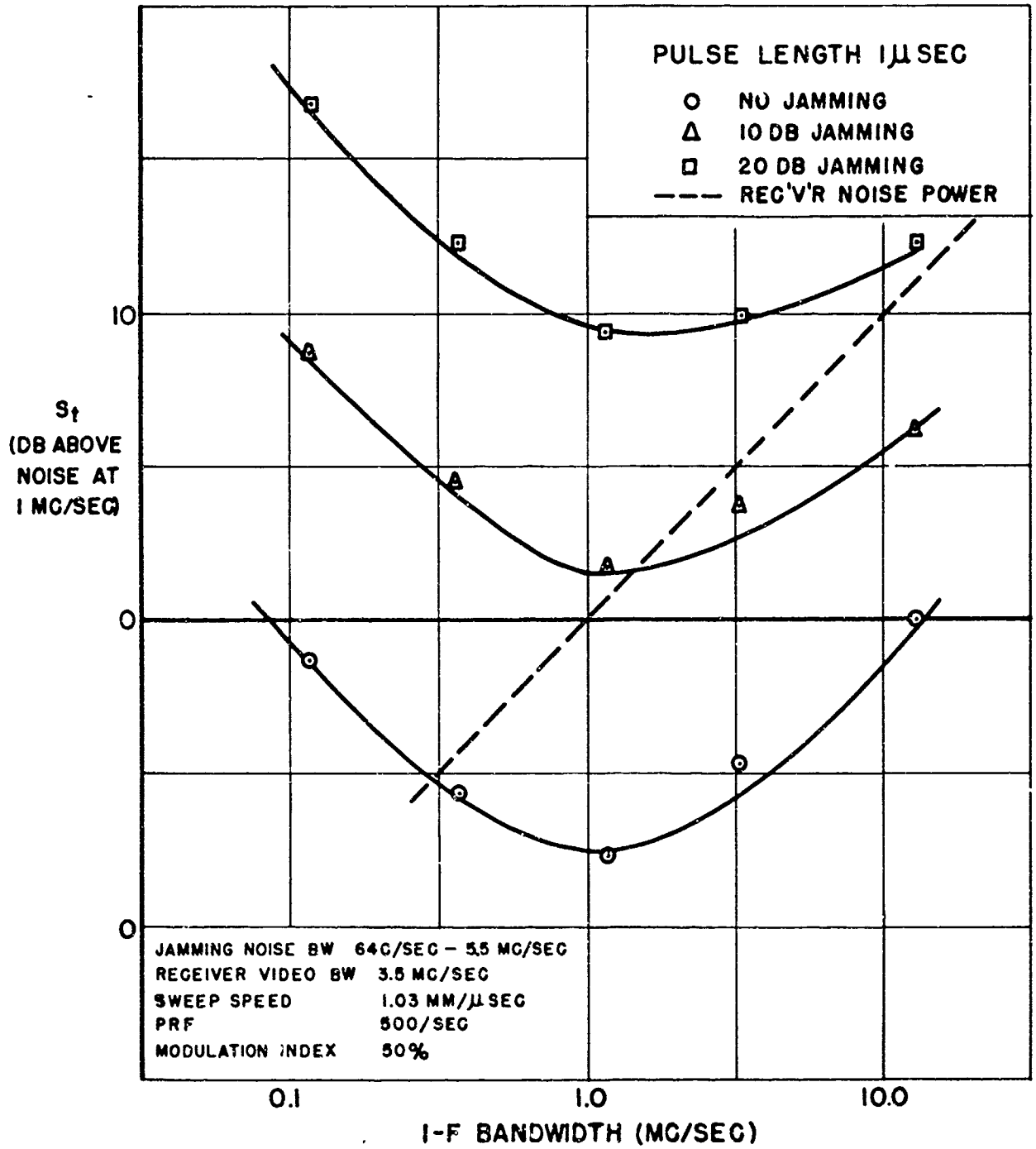


FIG. 13 THRESHOLD DEPENDENCE ON I-F BANDWIDTH

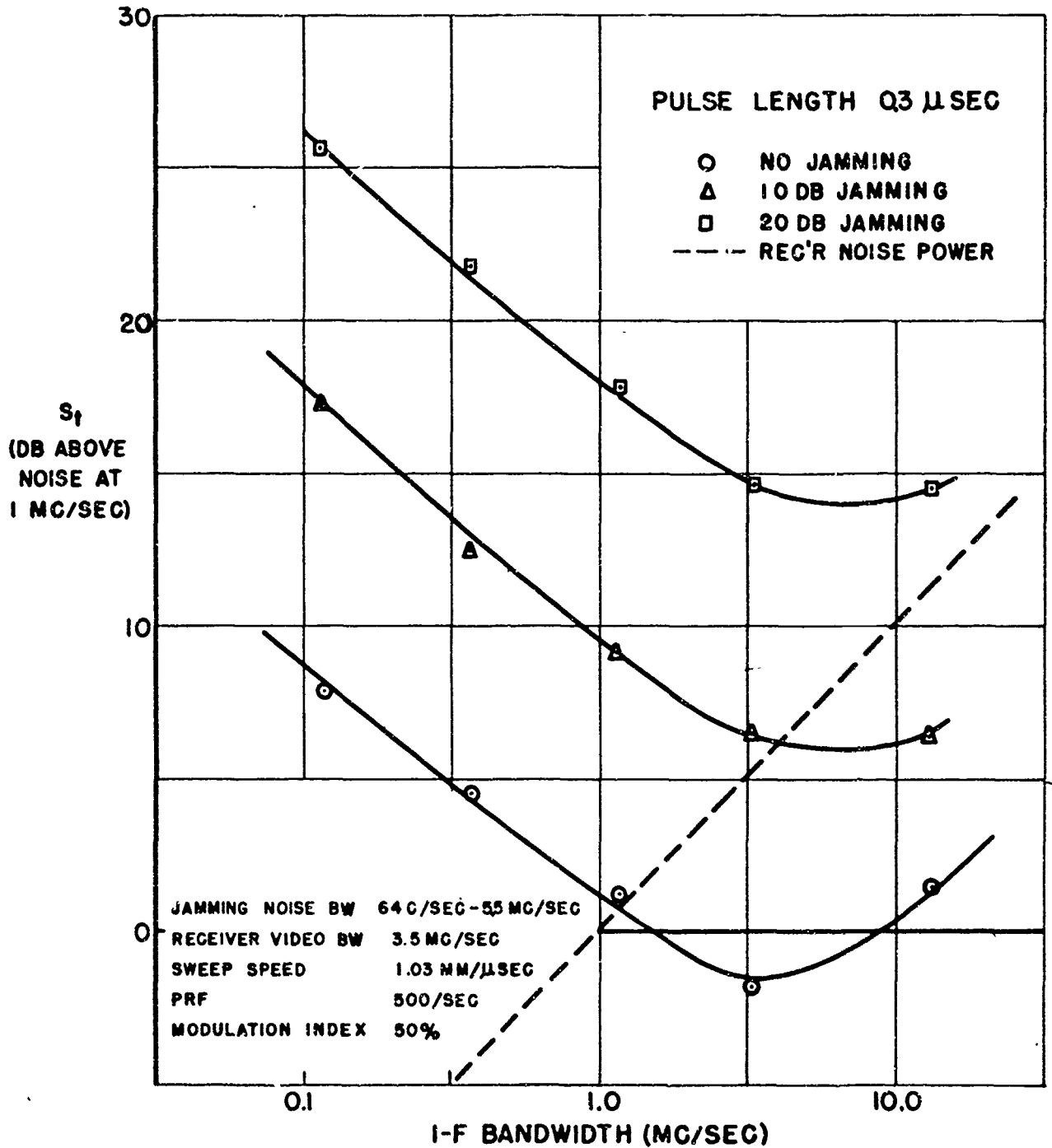


FIG. 14 THRESHOLD DEPENDENCE ON I-F BANDWIDTH

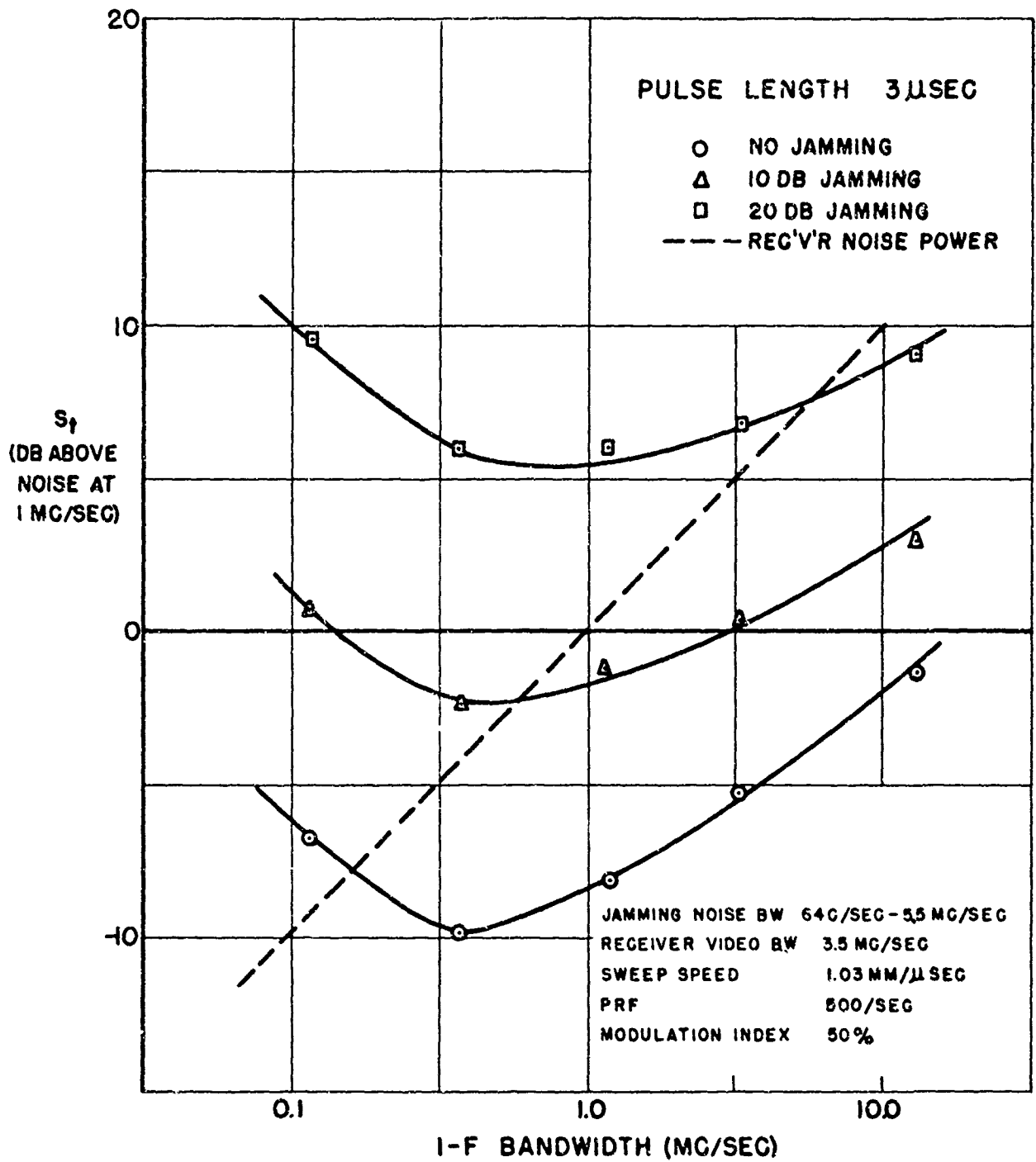


FIG. 15 THRESHOLD DEPENDENCE ON I-F BANDWIDTH

2.01

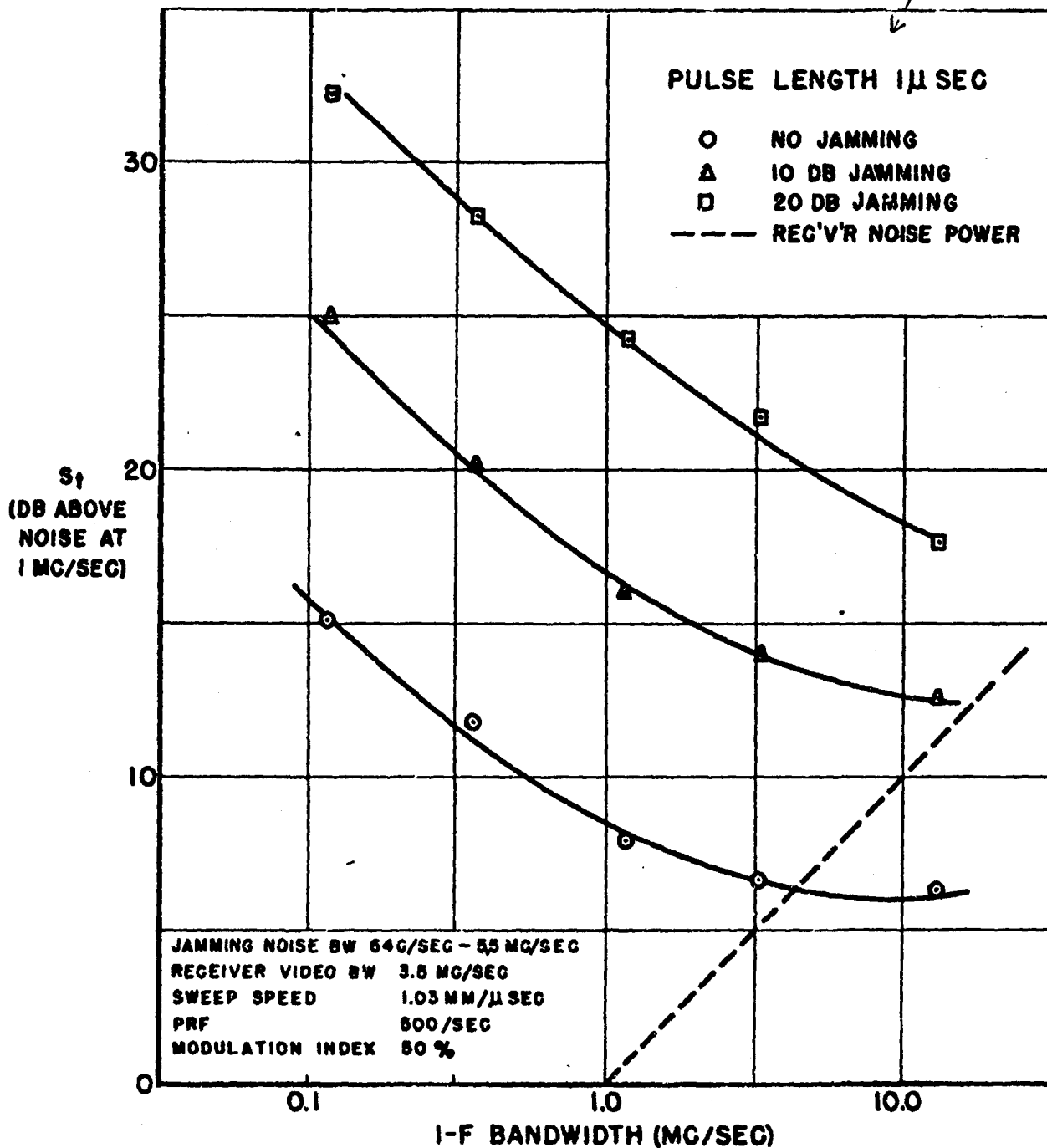


FIG. 16 THRESHOLD DEPENDENCE ON I-F BANDWIDTH

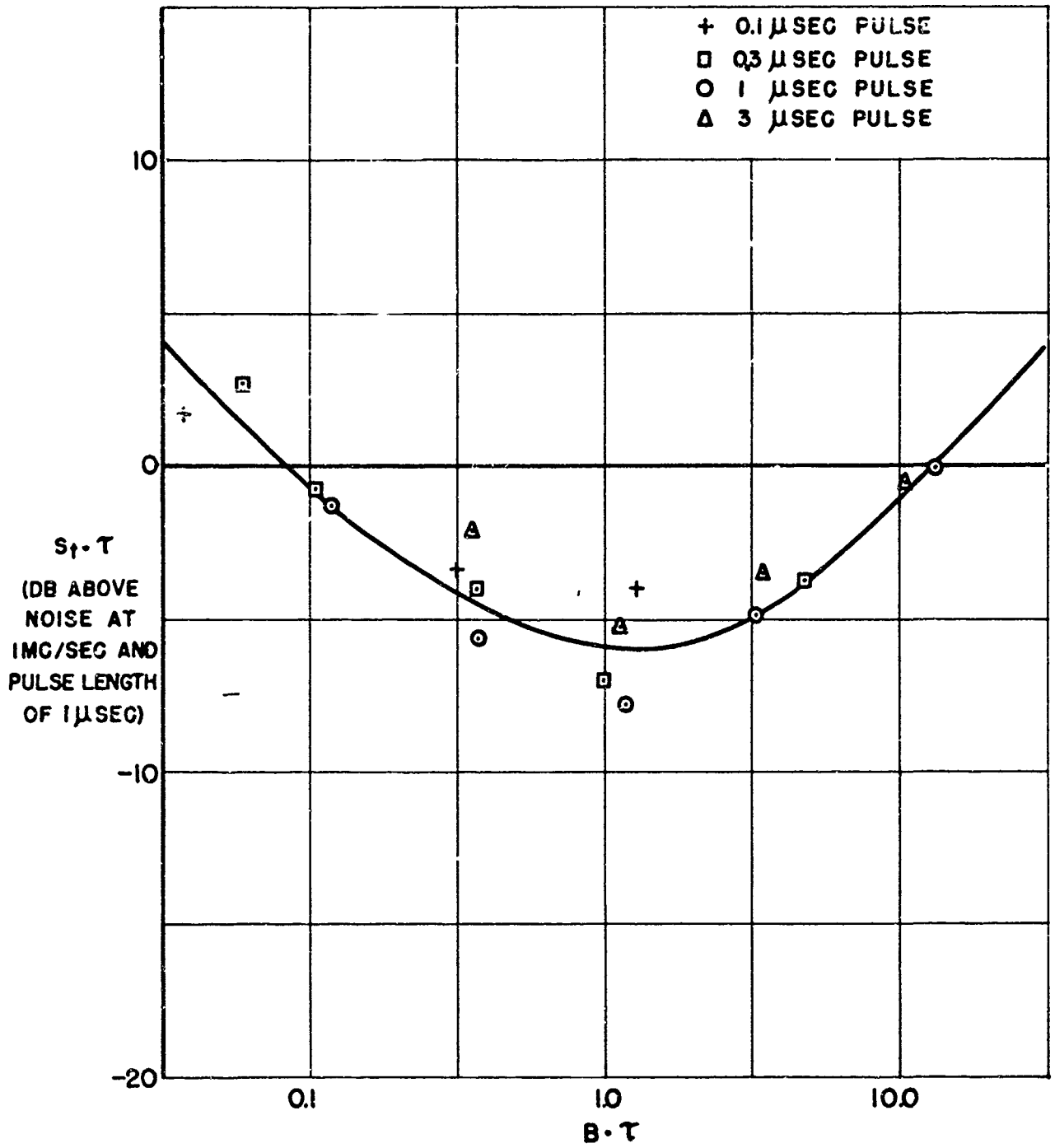


FIG. 17 UNIVERSAL SIGNAL THRESHOLD CURVE

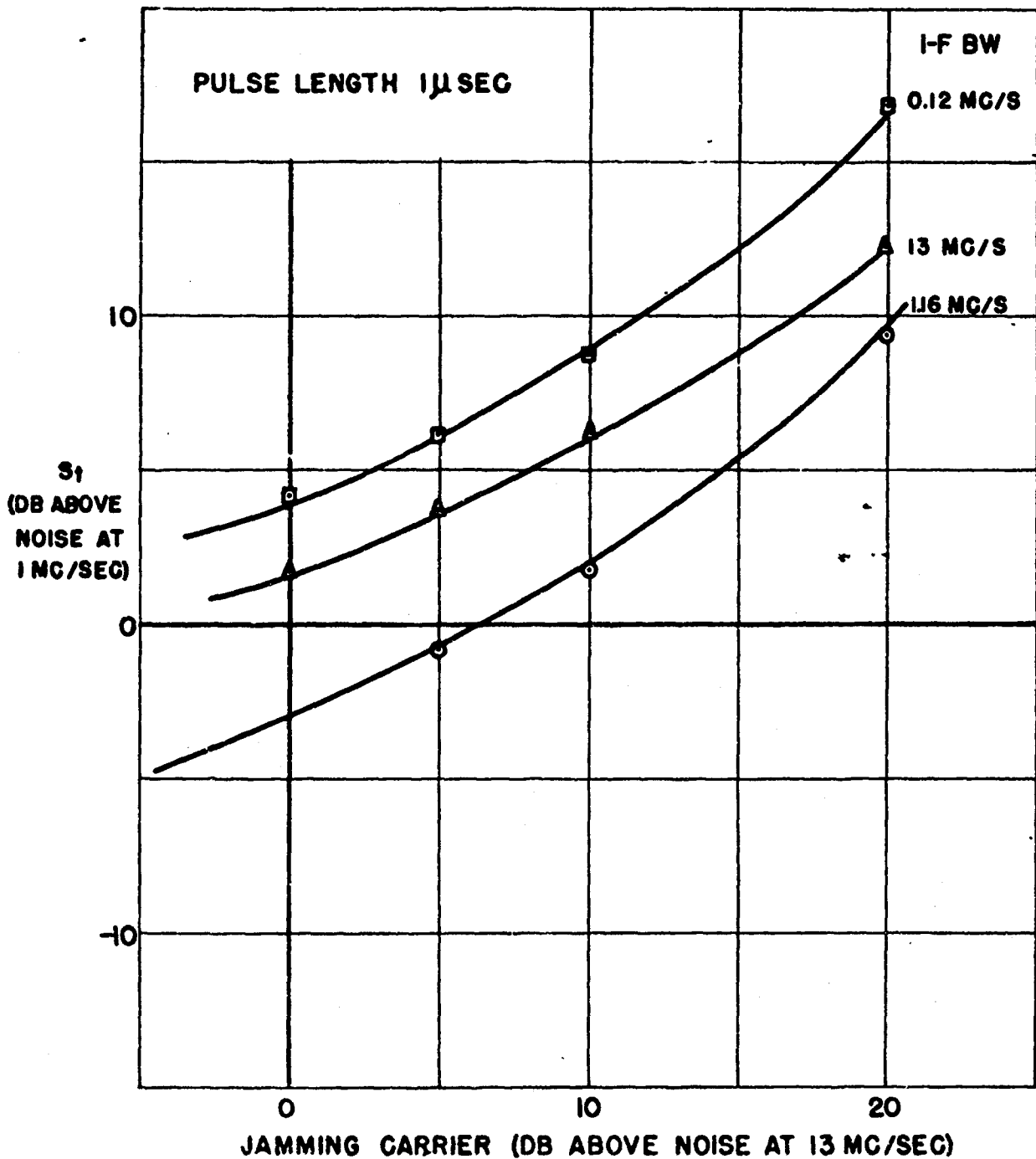


FIG. 18 DEPENDENCE OF S_1 ON JAMMING POWER

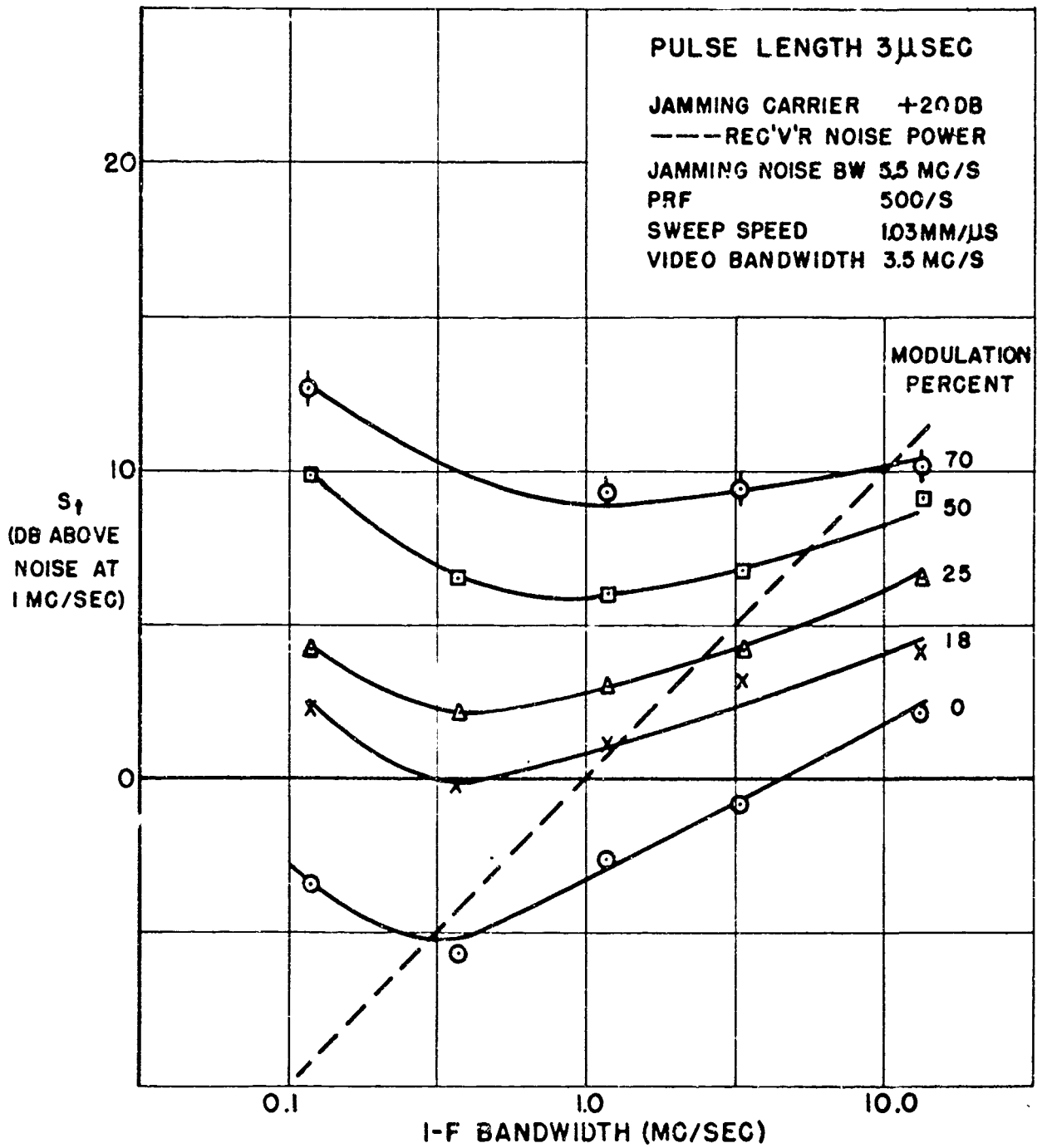


FIG. 19 EFFECT OF MODULATION INDEX ON SIGNAL VISIBILITY

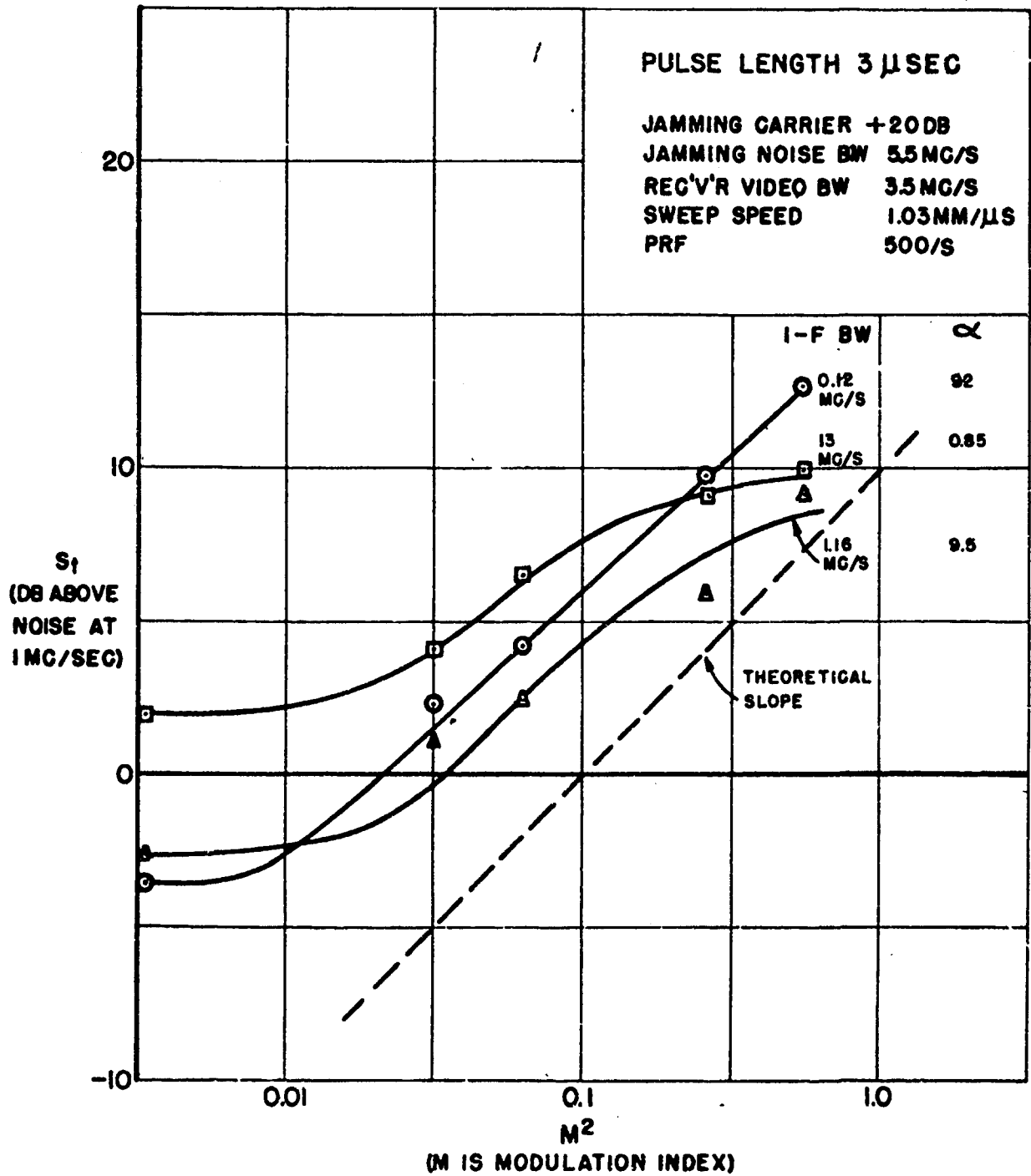


FIG. 19 a SECTIONS THROUGH FIG. 19

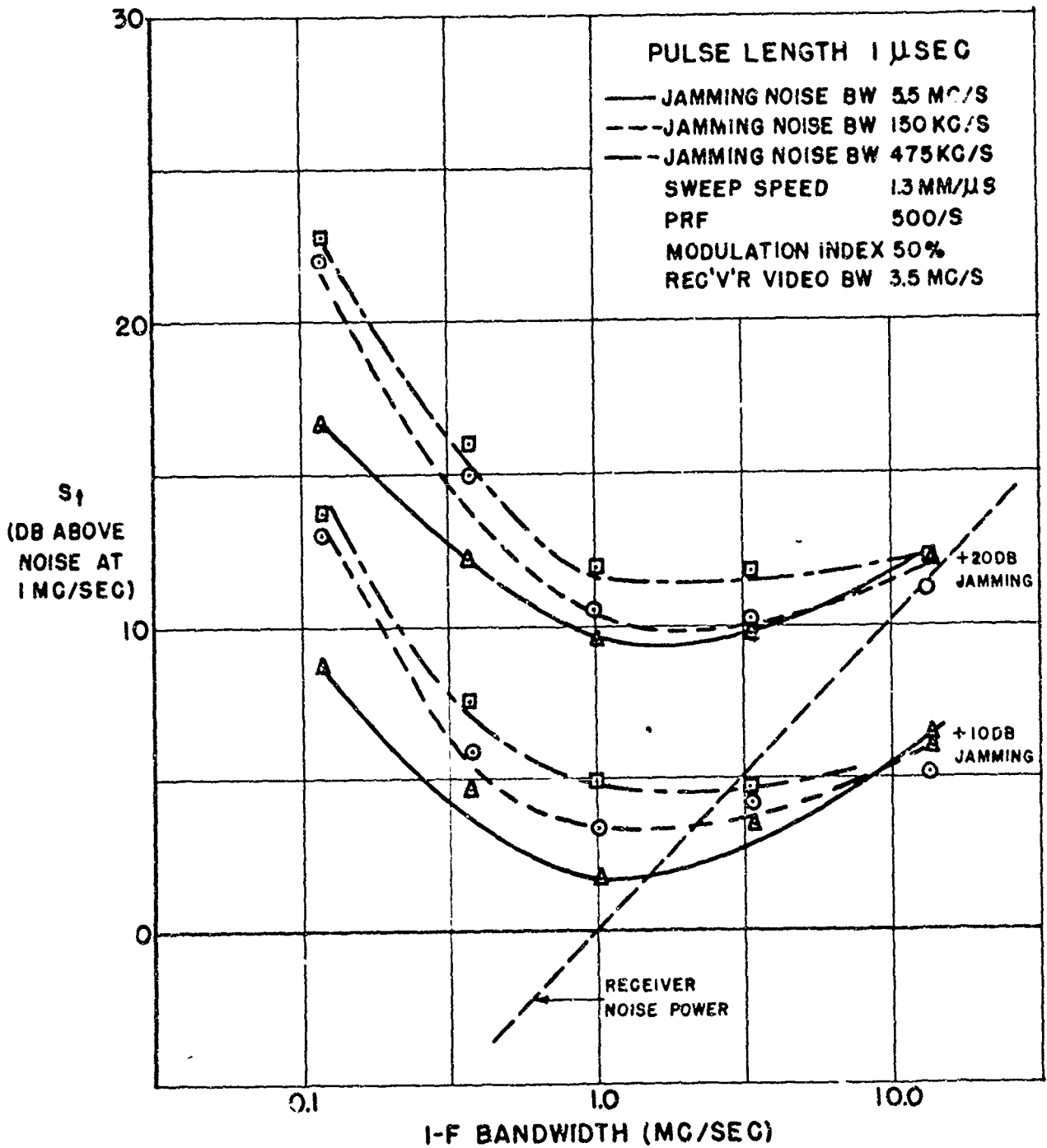


FIG. 20 EFFECT OF CHANGE OF JAMMING NOISE BANDWIDTH

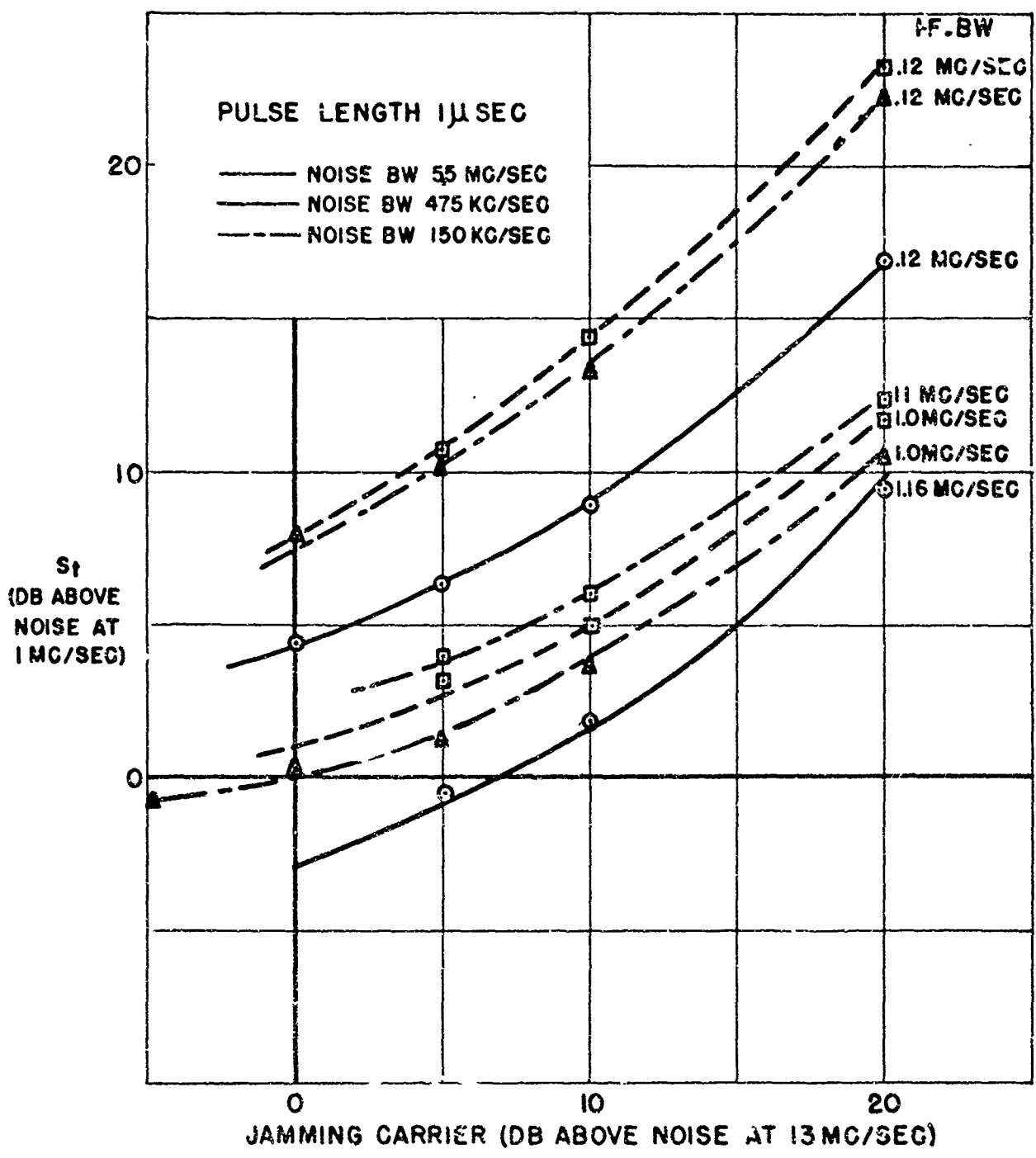


FIG. 21 S_f DEPENDENCE ON JAMMING POWER

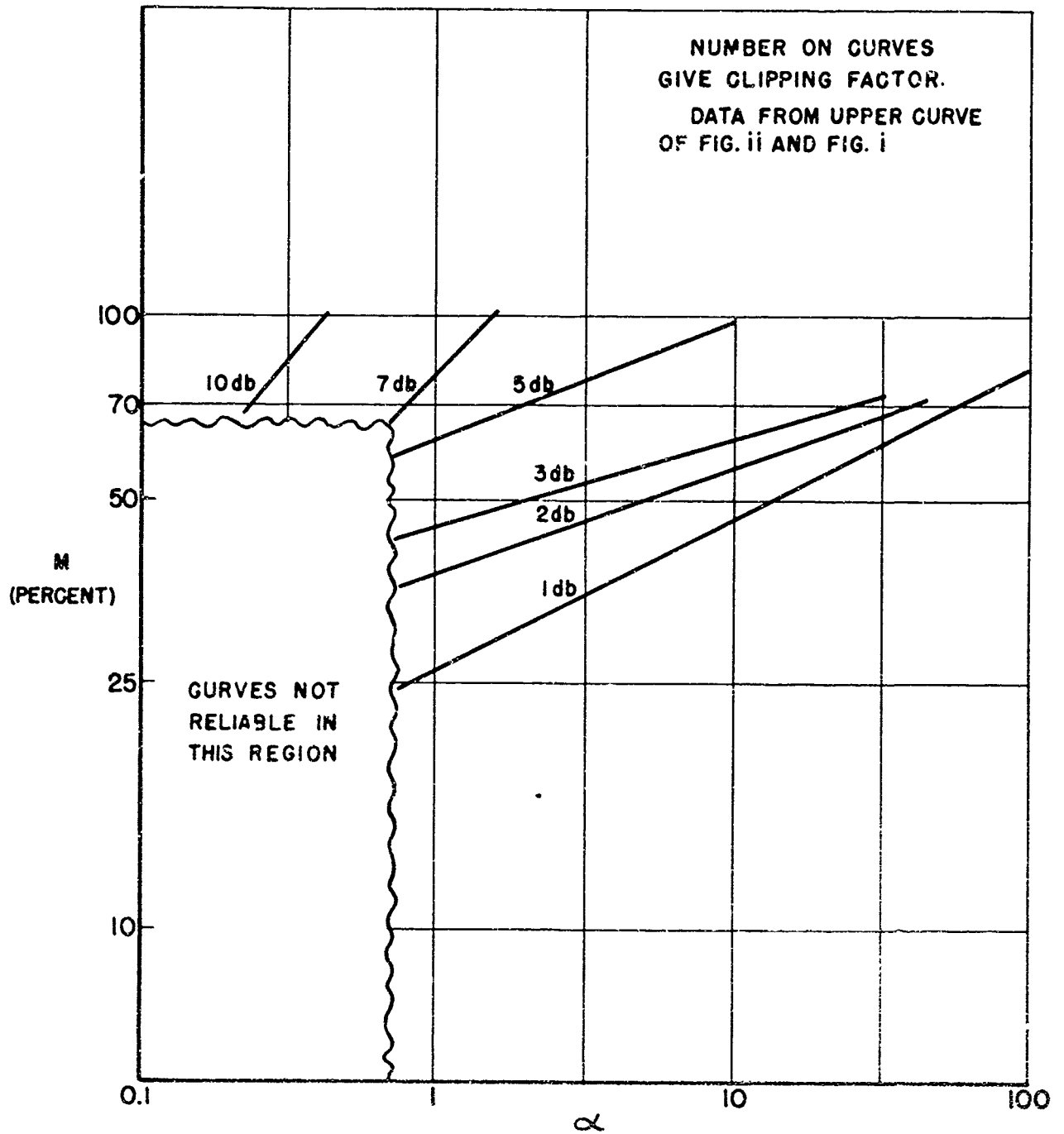


FIG. 22 CONTOURS OF CONSTANT F_c